ISSN 1949-8454 (online)

World Journal of *Biological Chemistry*

World J Biol Chem 2022 March 27; 13(2): 35-65

Published by Baishideng Publishing Group Inc

WJBC

World Journal of Biological Chemistry

Contents

Bimonthly Volume 13 Number 2 March 27, 2022

MINIREVIEWS

ORIGINAL ARTICLE

Basic Study

World Journal of Biological Chemistry

Bimonthly Volume 13 Number 2 March 27, 2022

Contents

ABOUT COVER

Editorial Board Member of *World Journal of Biological Chemistry*, Dr. Manoj Kumar Gupta, PhD, Postdoctoral Fellow, Department of Computational Biology for Individualised Infection Medicine, Centre for Individualised Infection Medicine (CiiM) & TWINCORE, joint ventures between the Helmholtz-Centre for Infection Research (HZI) and the Hannover Medical School (MHH), Feodor-Lynen-Str. 7, 30625 Hannover, Germany. mkg21@helmholtz-hzi.de

AIMS AND SCOPE

The primary aim of the *World Journal of Biological Chemistry* (*WJBC*, *World J Biol Chem*) is to provide scholars and readers from various fields of biological chemistry a platform to publish high-quality basic and clinical research articles and communicate their research findings online.

WJBC mainly publishes articles reporting research results and findings obtained in the field of biological chemistry and covering a wide range of topics including bioenergetics, cell biology, chromosomes, developmental biology, DNA, enzymology, extracellular matrices, gene regulation, genomics, glycobiology, immunology, lipids, membrane biology, metabolism, molecular bases of disease, molecular biophysics, neurobiology, plant biology, protein structure and folding, protein synthesis and degradation, proteomics, and signal transduction.

INDEXING/ABSTRACTING

The *WJBC* is now abstracted and indexed in PubMed, PubMed Central, Reference Citation Analysis, China National Knowledge Infrastructure, China Science and Technology Journal Database, and Superstar Journals Database.

RESPONSIBLE EDITORS FOR THIS ISSUE

NAME OF JOURNAL
World Journal of Biological Chemistry

ISSN
ISSN 1949-8454 (online)

LAUNCH DATE
July 26, 2010

FREQUENCY
Bimonthly

PUBLICATION DATE
March 27, 2022

World Journal of Biological Chemistry

Submit a Manuscript: https://www.f6publishing.com

World J Biol Chem 2022 March 27; 13(2): 35-46

DOI: 10.4331/wjbc.v13.i2.35

ISSN 1949-8454 (online)

MINIREVIEWS

LIN28A: A multifunctional versatile molecule with future therapeutic potential

Kenneth Wu, Tauseef Ahmad, Rajaraman Eri

Specialty type: Biochemistry and molecular biology

Provenance and peer review: Invited article; Externally peer reviewed.

Peer-review model: Single blind

Peer-review report's scientific quality classification

Grade A (Excellent): 0
Grade B (Very good): 0
Grade C (Good): C
Grade D (Fair): 0
Grade E (Poor): 0

P-Reviewer: Yang YZ, China

Received: March 27, 2021
Peer-review started: March 27, 2021
First decision: July 27, 2021
Revised: September 6, 2021
Accepted: March 4, 2022
Article in press: March 4, 2022
Published online: March 27, 2022

Kenneth Wu, Tauseef Ahmad, Rajaraman Eri, Department of Laboratory Medicine, School of Health Sciences, College of Health and Medicine, University of Tasmania, Launceston, Tasmania 7250, Australia

Corresponding author: Rajaraman Eri, DVM, PhD, Associate Professor, Department of Laboratory Medicine, School of Health Sciences, College of Health and Medicine, University of Tasmania, Health Sciences Building (Newnham-C), 2nd Level, Room M216, Launceston, Tasmania 7250, Australia. rajaraman.eri@utas.edu.au

Abstract

An RNA-binding protein, LIN28A was initially discovered in nematodes *Caenorhabditis elegans* and regulated stem cell differentiation and proliferation. With the aid of mouse models and cancer stem cells models, LIN28A demonstrated a similar role in mammalian stem cells. Subsequent studies revealed LIN28A's roles in regulating cell cycle and growth, tissue repair, and metabolism, especially glucose metabolism. Through regulation by pluripotency and neurotrophic factors, LIN28A performs these roles through *let-7* dependent (binding to *let-7*) or independent (binding directly to mature mRNA) pathways. Elevated LIN28A levels are associated with cancers such as breast, colon, and ovarian cancers. Overexpressed LIN28A has been implicated in liver diseases and Rett syndrome whereas loss of LIN28A was linked to Parkinson's disease. LIN28A inhibitors, LIN28A-specific nanobodies, and deubiquitinases targeting LIN28A could be feasible options for cancer treatments while drugs upregulating LIN28A could be used in regenerative therapy for neuropathies. We will review the upstream and downstream signalling pathways of LIN28A and its physiological functions. Then, we will examine current research and gaps in research regarding its mechanisms in conditions such as cancers, liver diseases, and neurological diseases. We will also look at the therapeutic potential of LIN28A in RNA-targeted therapies including small interfering RNAs and RNA-protein interactions.

Key Words: *Let-7*; Differentiation; Proliferation; Cancer; Inflammation

Core Tip: The overexpression of LIN28A has been correlated with a number of tumours and a higher risk of relapse in cancer patients. Therefore, LIN28A could be developed as a prognostic indicator. With an increasing understanding of its roles in the pathological context, LIN28A has also become a promising therapeutic target for cancer treatment and regenerative therapy for neuropathies.

Citation: Wu K, Ahmad T, Eri R. LIN28A: A multifunctional versatile molecule with future therapeutic potential. *World J Biol Chem* 2022; 13(2): 35-46
URL: https://www.wjgnet.com/1949-8454/full/v13/i2/35.htm
DOI: https://dx.doi.org/10.4331/wjbc.v13.i2.35

INTRODUCTION

First discovered in nematodes *Caenorhabditis elegans* (*C. elegans*) in 1997, the LIN28A (commonly referred to as LIN28 in some literature) protein is predominantly localised in the cytoplasm but can travel back and forth between the nucleus and cytoplasm. It was noted to be highly expressed during embryogenesis but gradually diminished to absent expression in adulthood in nematodes[1]. In humans, the absent expression was found to be only true in lung epithelium but it remains expressed during adulthood in certain cell or tissue types such as erythrocytes, renal epithelia of the loop of Henle and collecting ducts, cardiac muscle, and skeletal muscle[2]. Nonetheless, examination of LIN28 homologues in humans, mice, and *Drosophila* demonstrated its typical expression in undifferentiated and pluripotent cells, especially in embryonic stems cells (ESCs), then it is downregulated in response to development and differentiation. These findings suggested that LIN28A was involved in cellular development and differentiation. In fact, increased LIN28 expression has been associated with less differentiated and more aggressive tumours[2].

Invertebrates such as *C. elegans* and *D. melanogaster* possess a single *LIN28* gene whereas all vertebrates possess two LIN28 paralogs. LIN28's structure includes two RNA-binding domains, a N-terminal cold-shock domains (CSD), and a cysteine cysteine histidine cysteine (CCHC) zinc knuckle domains (ZKD) (Figure 1). LIN28 is regarded as the sole animal protein to possess the unique combination of a CSD and a C-terminal ZKD and has been implicated in promoting self-renewal and delaying differentiation, that resulted in proliferation of stem cells. Contrarily, its loss-of-function resulted in increased stem cell differentiation[2]. Its role in mammalian stem cells was elucidated in the early 2000s through studies such as human LIN28 being used to reprogram somatic fibroblasts into pluripotent stem cells[1]. These studies eventually demonstrated that LIN28A could bind to *let-7* gene to repress its expression in regulating translation. This binding was observed in a similar mechanism in *C. elegans*[1]. Thus, the findings had validated LIN28A's conserved role in stem cell self-renewal and differentiation.

In recent years, other roles of LIN28A have been linked to wound healing and tissue repair, cell growth and metabolism, and carcinogenesis while the signalling pathways have become more complex. In this review, we will elaborate on recent findings regarding the mechanisms and roles of the LIN28A protein in physiological functions and pathological processes. Subsequently, we will examine how these findings have translated into RNA-targeted therapies and drugs targeting protein interactions involving LIN28A in the treatment of cancer and other diseases.

SIGNALLING AND LET-7 PATHWAYS OF LIN28A

Regulatory signals

In vertebrates, an important intrinsic signal in downregulating LIN28A would be the microRNA-*125a* (miRNA-*125a*)[3]. In contrast, pluripotency factors such as Sox2, Nanog, and Tcf3 can promote *LIN28A* expression. Among these factors, Sox2 is regarded the most essential in this promotion of expression based on a Bayesian probabilistic network modelling of single-cell gene expression[3]. In addition, inhibition of Dot1L H3K79 histone methyltransferase indirectly upregulates LIN28A[3]. Extrinsic signalling has been demonstrated in *C. elegans*: Nuclear receptor *daf-12* transmits signals from steroid hormones to LIN28A, and *in vitro*: Homologous retinoic acid and oestrogen receptors downregulate LIN28A[3]. However, it is unclear if similar extrinsic signalling occurs in mammals.

Another signalling pathway involves brain-derived neurotrophic factor (BDNF) that initially activates extracellular signal-regulated protein kinase (Erk), which in turn mediates mitogen-activated protein kinase (MAPK) phosphorylation of transactivation response element RNA-binding protein (TRBP), an RNA-binding cofactor of the Dicer enzyme[4]. The act of phosphorylation decreased Merlin binding, which impedes polyubiquitination and proteasomal degradation of TRBP. Subsequently, BDNF can

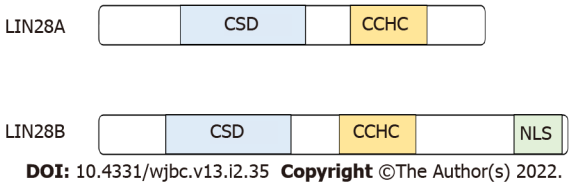

DOI: 10.4331/wjbc.v13.i2.35

Figure 1 Structure of LIN28 protein. LIN28 paralogs in vertebrates contain relatively conserved cold-shock domains and cysteine cysteine histidine cysteine. LIN28B contains a nuclear localisation signal at the end and is slightly longer than LIN28A. CSD: Cold-shock domains; NLS: Nuclear localisation signal; CCHC: Cysteine cysteine histidine cysteine.

stabilise and elevate levels of LIN28A *via* co-association with TRBP. An interesting finding was this MAPK-mediated TRBP phosphorylation and induction only targeted LIN28A but not its paralog, LIN28B. Hence, the BDNF-MAPK pathway induces LIN28A for physiological functions connected to dendritic spine growth and peritoneal macrophage survival as part of the trophic responses[4].

LIN28A has been found to be involved in several feedback loops. Firstly, it has been ascertained that LIN28A inhibits *let-7* expression while *let-7* itself binds to mRNA of LIN28A to downregulate LIN28A expression, which establishes a double negative feedback loop[3]. Secondly, LIN28A can derepress c-Myc *via let-7* inhibition, then c-Myc can upregulate LIN28A expression, which establishes a positive feedback loop. Thirdly, an initial inflammatory signal activates nuclear factor kappa-light-chain-enhancer (NF-κB) that elevates interleukin-6 (IL-6) levels that is also elevated by LIN28A's inhibition of *let-7*. The increased IL-6 levels activate NF-κB, which completes the positive feedback loop[1].

Let-7 pathways

In *C. elegans*, the mechanisms in regulating its four developmental stages can be divided into *let-7* dependent and *let-7* independent pathways[2]. The former involves LIN28 promoting the expression of *lin-41* by repressing *let-7*, which in turn reduces binding of *let-7* to LIN28A mRNA. Therefore, either LIIN28A or *let-7* can suppress one another in forming a bistable switch. The latter involves *lin-4* targeting LIN28 which upregulates hunchback-like protein-1 (hbl-1) that inhibits *let-7*[2]. Interestingly, the latter may be utilised in mammalian systems which would further corroborate the conserved role of LIN28 but there does not appear to be any concrete findings.

In this review, these two divisions are adapted to elaborate on LIN28A mechanisms in humans.

Let-7 dependent pathways: In the nucleus, LIN28A binds primary *lethal-7* (pri-*let-7*) synergistically with RNA-binding protein musashi 1 (MSI1) to block *let-7* processing *via* a miRNA-processing enzyme Drosha (Figure 1)[2]. In the cytoplasm, LIN28A binds precursor *lethal-7* (pre-*let-7*) to competitively block the Dicer processing (another microRNA-processing enzyme) to prevent the formation of mature *let-7*. Then, LIN28A recruits terminal uridylyl transferase 4 (TUT4) for the oligo-uridylation of pre-*let-7*; this process prevents the cleavage of pre-*let-7* by Dicer and acts as a signal for exonuclease DIS3L12 for its degradation (Figure 2)[2].

In terms of structural significance of LIN28, the pri-*let-7* pathway appears not be as expounded as much as the pre-*let-7* pathway. In the nucleus, it is hypothesised that the LIN28A's CSDs bind with increased affinity to pri-*let-7*[5] to block cleavage by Drosha which prevents Drosha-mediated processing[6]. In a related study, LIN28 has demonstrated another mechanism similar to that of its counterpart, LIN28B: The histone H3K4 methyltransferase can mono-methylate LIN28A; which appears to enable its localisation in the nucleus and especially nucleolus, and increases its binding affinity to pri-*let-7*[7].

In the cytosol, LIN28's ZKDs can recognise and bind to GGAG or GGAG-like motifs in pre-*let-7*'s terminal loop to compete with Dicer in inhibiting Dicer-mediated processing and TUTase would then be recruited[6]. Furthermore, TUT4 and TUT7 also possess CCHC Zn knuckles that are required in pre-*let-7* oligouridylation[1]. While initial research only involved mechanisms surrounding binding of LIN28A to *let-7* (*let-7* dependent), subsequent research examined binding of LIN28A to specific mRNAs (*let-7* independent).

Let-7 independent pathways: Several small-scale studies have isolated a number of potential LIN28 mRNA targets and most of them are mature mRNA and involved in cell cycle regulation, metabolism, or formation of ribonucleoprotein complexes (Table 1)[2,8]. In first understanding how LIN28 recognises these targets, three genome-wide studies determined rather divergent consensus sequences amongst the targets despite such large data sets[2].

Furthermore, Cho *et al*[9] located their consensus sequence within the terminal loop of small hairpins [2]. Wilbert *et al*[10] noted their targets' consensus sequences of interest were enriched in single-stranded RNA (ssRNA) within the hairpin and other loop structures whereas Qiu *et al*[11] found that their targets were enriched in LIN28-containing polysome fractions[2]. Then, Hafner *et al*[8] discovered LIN28 preferentially binds to ssRNA containing a uridine-rich element and guanosines when embedded in secondary structure[8]. However, the presence of this secondary structure may not be significant due

Table 1 Classes of mRNA targets[2]

Cell cycle regulation	RNA-binding proteins	Histone components	Glucose metabolism	Early embryogenic genes
Cyclin A	hnRNP F	Histone H2A	IGF receptor	*Sox2*
CDK4	TDP-43	Histone H4H	Insulin receptor	*Sall4*
CCNB1	TIA-1	Linker histone H1FX	HMGA2	*Oct4*

IGF: Insulin-like growth factor 1. Citation: Tsialikas J, Romer-Seibert J. LIN28: roles and regulation in development and beyond. *Development* 2015; **142**: 2397-2404. Copyright© The Authors 2015. Published by The Company of Biologists Ltd.

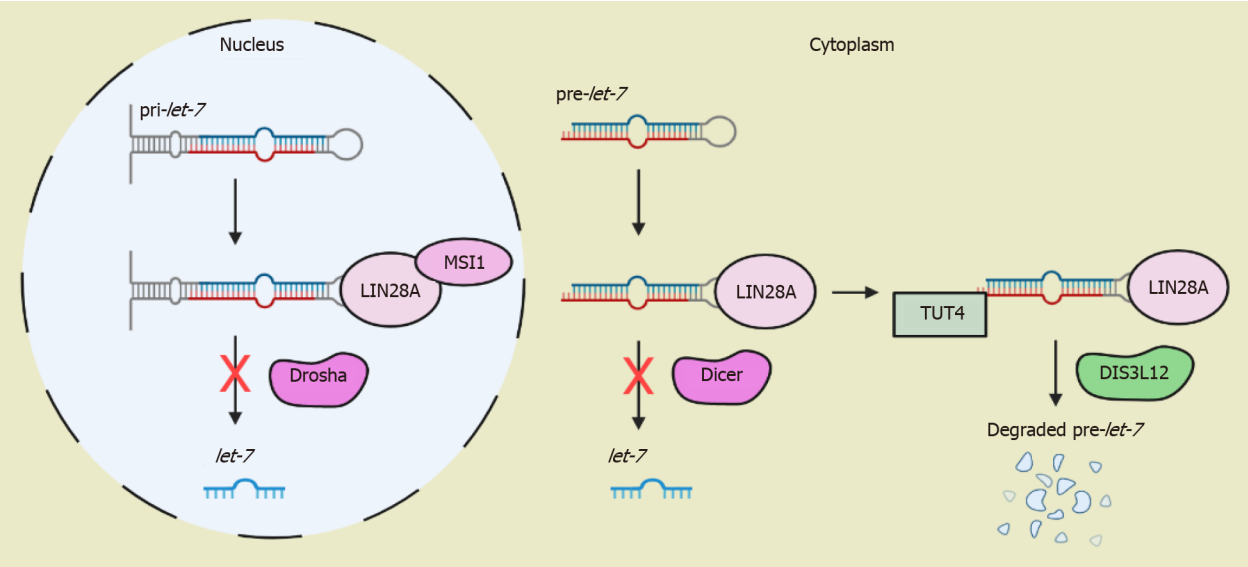

DOI: 10.4331/wjbc.v13.i2.35

Figure 2 Molecular pathways of LIN28A/*let-7* axis. LIN28A binds to pri-*let-7* in the nucleus to prevent its processing by Drosha and to pre-*let-7* in the cytoplasm to prevent Dicer processing as well as facilitate its degradation.

to variation in stem length and loop size and lack of formal statistical analysis.

Despite the divergent consensus sequences, similarities such as the ssRNAs and loop structures indicate that the recognition mechanisms for LIN28 to these RNAs is gradually being uncovered. With an improved understanding of how LIN28 binds to its targets, researchers also looked at the significance of its pathways in humans.

PHYSIOLOGICAL FUNCTIONS

Cell differentiation and cell cycle

LIN28A is most prominently known as a regulator of cell renewal and differentiation. Multiple studies highlight this evolutionarily conserved role in ESCs and trophoblast stem cells. In fact, Li *et al*[12] reported that *PpCSP1* (a homologue of LIN28) can revert differentiated leaf cells to stem cells in moss *Physcomitrella patens*; indicating that LIN28's role involving cell differentiation extends beyond the animal kingdom[12]. In the classical *let-7* dependent pathway, LIN28 can suppress *let-7* biogenesis to promote ESC differentiation[13]. In the *let-7* independent pathway, LIN28 can impede translation of mRNAs such as high mobility group AT-Hook 2 (HMGA2) to either prevent its disruption of ESC differentiation or its effect of uncontrolled cell proliferation and apoptosis when HMGA2 is allowed to accumulate[13].

Similarly, LIN28A utilises the classical pathway to regulate trophoblast differentiation and neural precursor cells (NPCs) proliferation. To retain pluripotency in trophoblast progenitors, LIN28A increases; suppressing *let-7* whereas to initiate their differentiation, LIN28 decreases; enabling *let-7* to mature[14]. Proliferation of NPCs and increase in brain size is promoted by Sox2 through LIN28A. Notably, LIN28 has been suggested to be sufficient in rescuing NPC proliferation and neurogenic deficits in the absence of Sox2[15]. In facilitating cell cycle progression, LIN28A can promote expression of cyclin D1 (CCND1) and cell division cycle 25 homolog A (CDC25A) by inhibiting miRNA biogenesis (

let-7 dependent) and bind to cell cycle regulatory mRNAs such as cyclin-dependent kinase 2 (CDK2) to promote their translation (*let-7* independent)[16].

Cell and tissue repair

Overexpression of LIN28A improves tissue repair such as digit repair, pinnal tissue repair, epidermal hair regrowth, and axon regeneration in both peripheral nervous system and central nervous system (CNS)[17,18]. The LIN28A/*let-7* axis was implicated in these various tissues. Firstly, LIN28A enhances proliferation of connective tissue and bone for digit repair and mesenchymal tissue for pinnal tissue repair[17]. Secondly, it prolongs anagen phases (the active phase of the hair growth cycle) in hair follicles to promote hair regrowth[17]. Lastly, it represses glial *let-7* miRNAs which can inhibit axon regeneration by targeting nerve growth factor in Schwann cells; the inhibitory effects of neuronal *let-7* miRNAs on axon regeneration are uncertain[18].

In addition, LIN28 manipulates reprogramming factors such as Klf4, c-Myc, and Sox11 to enable mature CNS neurons to regain their ability to support axon regeneration, with the possible involvement of Akt-mTOR and GSK3β pathways[18]. Corroborating studies indicate that LIN28 can also functionally replace c-Myc, one of the Yamanaka factors responsible in reprogramming mature cells into induced pluripotent stem cells, and recruit Tet1 to regulate DNA methylation and gene expression. These properties enable LIN28 to influence epigenetic remodelling in facilitating axon regeneration.

On the other hand, the LIN28-mediated metabolic enhancements such as enhanced glycolysis could meet the higher energetic demands of anabolic biosynthesis and cell migration in accelerating tissue repair. However, it was observed that *let-7* repression alone is insufficient to replicate this facet of LIN28's role; indicating that the *let-7*independent pathway is imperative in tissue repair[17].

Growth and metabolism

LIN28A is one of the elements affecting organismal mortality and growth including the onset of puberty. Constitutive loss or embryonic deficiency of *LIN28A* has been associated with perinatal lethality and dwarfism. While diminished organogenesis contributed to dwarfism, the exact cause of the LIN28-deficient perinatal lethality is currently unknown[19]. An interesting finding is *LIN28A* acts earlier on organismal growth compared to its paralog *LIN28B*, such that the impacts by the former's deletion are primarily restricted to foetal or early postnatal tissues and already manifest in utero[19]. However, the prenatal impacts can have life-long consequences, as described in Barker hypothesis, which states that epigenetic memory of poor foetal or infantile environment can become an important determinant of risk for major chronic diseases such as cardiovascular disease and type 2 diabetes[19].

In terms of skeletal muscle development, overexpression of *let-7* (due to decreased LIN28A) in skeletal muscle is capable of causing growth retardation[20]. Studies demonstrate that *let-7* can impede cell proliferation by downregulating insulin-like growth factor 1, an essential hormone in growth and development, and initiate cell cycle arrest by downregulating cell cycle factors such as CKD6 and CDC34. As a result, the activation, proliferation, and maturation of myosatellite cells (precursors to skeletal myocytes) are hindered[20]. Conversely, overexpression of LIN28A is associated with increased body size and delayed onset of puberty. It is hypothesised that the LIN28A/*let-7* axis influences the hypothalamic-pituitary gland axis through secretion of hormones such as growth hormone and gonadotropin releasing hormone, which are required for growth and initiating the puberty onset[21].

In both *in vitro* and *in vivo* models, LIN28A overexpression demonstrates elevated glucose uptake and glycolysis. This is achieved by LIN28 increasing the levels of hexokinase 2, the enzyme considered as the rate-limiting step and the first step in glycolysis[22]. Concurrently, LIN28 overexpression also increased PTEN-induced kinase 1 and mitofusin 2, which mediates mitochondrial recycling and thus, reduce oxygen consumption in these LIN28-overexpressed cells such as Hep3B cells[22]. However, LIN28-overexpressed MEF isolated from mice presented an increased oxygen consumption; intimating that LIN28A's effect on oxygen consumption may depend on cell type. Nonetheless, LIN28 catalyses a shift from oxidative metabolism towards glycolytic metabolism. Now that LIN28A has been established as a regulator of glucose metabolism; increased LIN28A expression and thus, decreased expression of *let-7* led to normal glucose tolerance and an insulin-sensitised state, which lowered the risk of obesity and diabetes[23].

PATHOLOGICAL IMPLICATIONS

LIN28A's various physiological roles have linked it to various pathological processes. Its relevance in cancers, especially of breast, ovarian, and colon tissue are covered extensively in comparison to diseases such as Friedrich's ataxia and Parkinson's disease.

Cancer

Being a regulator of cell proliferation and differentiation, LIN28 overexpression and reduced *let-7* expression is often correlated with certain cancers. It has been proven that downregulation of *let-7* miRNAs catalyses the derepression of oncogenes such as Ras and c-MYC, contributing to tumorigenesis

or metastasis (Table 2)[24,25]. Notably, these oncogenes play a role in cell differentiation and proliferation; the former resulting in activation of the RAS-mitogen-activated protein kinases (RAS-MAPK) pathway which leads to uncontrolled cell proliferation while the latter influences a multitude of pathways involved in cell cycle progression, cell proliferation and differentiation, cell adhesion, and metabolism[26]. Alternatively, LIN28A was involved in oncogenesis through other pathways such as the direct interaction with mRNA.

For example, LIN28A can bind to mRNA of bone morphogenetic proteins 4 (BMP4) to induce BMP4 overexpression, which stimulates cell proliferation and tumour growth in ovarian cancer[24]. Another example is LIN28 enhancing mRNA translation of human epidermal growth factor receptor 2 (HER2) and HMGA1, which promotes cell proliferation in breast cancer[24]. Therefore, LIN28A overexpression is typically associated with poor prognosis and a higher risk of relapse (Table 2)[25].

From a metabolic perspective, LIN28A promotes aerobic glycolysis in cancer cells by upregulating glycolysis-associated genes. Previously, it was thought that the insulin-Akt-mTor pathway was the primary cause but the pathway was not significantly impacted by LIN28A levels[27]. Further studies demonstrated LIN28A overexpression resulting in elevation of an important glycolytic enzyme, pyruvate dehydrogenase kinase 1 (PDK1). PDK1 inactivates pyruvate dehydrogenase, the enzyme that converts pyruvate to acetyl-coenzyme A in the Krebs cycle. This inhibits oxidative phosphorylation activity.

Consequently, cancer cells would undergo a metabolic switch from oxidative phosphorylation to aerobic glycolysis in normoxic conditions, *i.e.* Warburg effect, as part of cancer progression[27]. In addition, LIN28A has been demonstrated to bind with the mRNAs of sterol regulatory element-binding protein 1 (SREBP-1) and SREBP cleavage-activating protein (SCAP) to augment translation and maturation of SREBP-1. This promotes fatty acid synthesis, which in turn protects cancel cells from fatty acid-induced endoplasmic reticulum stress[28].

In understanding the pathophysiology of carcinogenesis, cancer stem cells (CSCs) in certain cancers such as breast, colon/colorectal, and ovarian cancers are examined. In colon cancer, LIN28A overexpression promotes proliferation of colon cancer cells by promoting the transition of cell cycle from S to G2/M phase[29] through upregulation of cell cycle factors such as cyclin A2[30]. In breast and ovarian cancer, LIN28A promoted the G0 or G1 transition instead through the *let-7* suppression and increase in expression of cell cycle factors such as CCND1 and CDK34 for breast cancer or CDK2 for ovarian cancer [16,31]. These findings suggest that LIN28A's regulatory control in the cell cycle differs from tissue to tissue.

There are a few studies stating that LIN28A stabilises RNA FBXL19-AS1 which sponges anti-oncogenic proteins such as miRNA-203 (in colorectal cancer) and WD Repeat Domain 66 (in breast cancer)[32,33]. Consequently, cell migration and invasion are no longer inhibited. Interestingly, a number of articles point towards its paralog LIN28B for being responsible in cell migration and invasion by decreasing *let-7* expression and activating the Wingless Integration 1 (Wnt)/ β-catenin pathway; leading to a significant reduction of E-cadherin levels but an elevation of vimentin levels; causing disruption of the epithelium which enables the migration of cancer cells from the primary site[34,35]. Furthermore, abnormal β-catenin-E-cadherin complexes could diminish cellular adhesion and epithelial cell interstitialisation, which are required in limiting cell growth and cell migration primarily through contact inhibition[35]. Consequently, cell migration and invasion are facilitated.

For ovarian cancer, its malignancy is exacerbated by LIN28A hindering the activity of cleaved caspase-3, caspase-7, and caspase-9. Thus, the DNA damage repair enzyme, poly adenosine diphosphate-ribose polymerase (PARP) cannot be cleaved, which inhibits cell apoptosis of these cancer cells[36]. A unique mechanism in LIN28-expressing ovarian cancer cells is their secretion of exosomes, which contain miRNAs such as miRNA-200 and miRNA-17-92 that are taken up by non-tumour cells [37]. Subsequently, they induce EMT with miRNA-200 inhibiting zinc finger E-box binding homeobox 1 (ZEB1) to derepress E-cadherin as well as miRNA-17-92 regulating CYP7B1 and E-cadherin expression to ultimately promote migration and invasion[38].

In contrast with the previous three cancers, overexpression of LIN28A and hence, downregulation of *let-7* expression impeded cell proliferation, migration, and cell cycle progression in gastric cancer cells [39]. In fact, LIN28A overexpression induced apoptosis of these cells. Neither the related study or current literature explain this inverse relationship and its mechanisms.

Liver diseases

In hepatitis, LIN28A plays an active role in the balancing of EMT for fibrosis with mesenchymal-to-epithelial transition (MET) for liver regeneration; both processes are vital for liver repair[40]. Firstly, one of LIN28A targets include miRNA-200c which decreases expression of Fas-associated phosphatase 1 in order to increase expression of a proto-oncogene, tyrosine-protein kinase Src kinase (Src) and stimulate liver fibrosis[40]. In addition, another target, miRNA-107 can modulate components of the IL-6 receptor (IL-6R) complex in order to downregulate expression of chemokine (C-C motif) ligand 2 (CCL2), that is an inflammatory chemokine elevated in chronic liver diseases such as hepatitis C. Therefore, miRNA-107 can inhibit IL-6 signalling in regulating the inflammatory response and to an extent, fibrosis[40]. Secondly, LIN28A's repression of *let-7* removes the latter's inhibitory effect on IL-6 so activation of SRC can now elevate IL-6 Levels to induce inflammation[40]. Consequently, LIN28A and its targets disrupt

Table 2 Clinical relevance of LIN28A in certain cancers[25]

Tissue	Primary tumour	Clinical Relevance of LIN28A
Breast	HER2 + tumour	Overexpression correlated with HER2 + tumours
Colon	Primary adenocarcinoma	Expressed in approximately 30% tumours
Kidney	Primary Wilms' tumour	Overexpressed in late stage
Lung	Small cell lung cancer	Loss increases *let-7* levels; inhibits cell cycle
Oesophagus	Primary human tumour	Expression linked to metastasis and poor prognosis
Ovary	Primary ovarian tumour	Knockdown increases *let-7* expression

Citation: Thornton JE, Gregory RI. How does Lin28 Let-7 control development and disease? *Trends Cell Biol* 2012; **22**: 474-482. Copyright© The Authors 2012. Published by Elsevier Ltd. All rights reserved.

the balance of the inflammatory response and prolong fibrosis, which can have detrimental effects such as cirrhosis, portal hypertension, and liver failure.

Chronic cirrhosis can lead to oncogenic transformation into hepatocellular carcinoma (HCC), considered the most common primary liver tumour and leading cause of cancer death in the world[41]. As with most LIN28-linked cancers, increased LIN28 and decreased *let-7* are involved in the unregulated cellular proliferation and enhanced metastatic ability[40,41].

Biliary diseases can refer to primary biliary cholangitis, an autoimmune destruction of small to medium-sized bile ducts are destroyed and primary sclerosing cholangitis, inflammation of bile ducts coupled with structuring and sclerosis[40]. Both conditions contribute to cholestasis but more importantly, both involve inflammation. Therefore, LIN28A is suggested to play a critical role in tissue repair and inflammation or progression to cholangiocarcinoma. This is supported by *in vitro* studies showing that *let-7* can regulate inflammatory processes by modulating expression of lipopolysaccharide (LPS) toll-like receptor of cholangiocytes[40], and mice with cholangiocarcinoma presenting with decreased *let-7* and increased LIN28B instead[42].

Other liver diseases include non-alcoholic fatty liver disease (NAFLD), which is characterised by steatosis due to excessive consumption of sugar and fats or certain medications; and polycystic liver disease (PCLD), which encompasses autosomal dominant or recessive disorders occurring in association with polycystic kidney diseases[40]. In NAFLD, a primary inflammatory regulator is the NF-κB which has been correlated with an elevation of LIN28 Levels, which would decrease *let-7* levels[43]. In PCLD, LIN28's influence is hypothesised through two findings: The cholangiocytes in PCLD possessing the ability to undergo EMT and majority of miRNAs that were part of the *let-7* family exhibited reduced expression in cystic cholangiocytes[40]. However, current literature does not elucidate LIN28's roles and mechanisms in PCLD.

Neurological diseases

Parkinson's disease is characterised by degeneration of the dopamine neurons in the midbrain's substantia nigra that results in tremors and stiffness. *In vitro*, loss of LIN28A yielded neural stem cells with absent dopamine neurogenic potential and diminished repair capacity as well as more vulnerable dopamine neurons when exposed to toxic environments. This indicates loss of LIN28A affected development of healthy and properly functional dopamine neurons[44]. Hence, this loss is correlated with the pathogenesis involving degeneration of neurons. Next, Rett syndrome is characterised by loss-of-function mutations in *MECP2* that results in intellectual and motor impairments. Proteomic analyses revealed that LIN28 overexpression repressed astrocyte differentiation and decreased synapse formation. This leads to defects in glial differentiation and neuronal maturation, which in turn impairs neurodevelopment and hence, creates a dysfunctional nervous system[45].

THERAPEUTIC APPROACHES

Considering LIN28A's various physiological functions and pathological roles, therapeutic approaches have been developed involving its pathways and pharmaceutical drugs. This review will focus on drugs or proteins that directly target LIN28A or those that target essential or related components in the LIN28/*let-7* axis.

Cancer

With regard to LIN28A inhibitors, studies have investigated compounds such as 1632, TPEN, and L171. Firstly, 1632 prevented LIN28 from interacting with *let-7*, which in turn enables *let-7* levels to rise to

avoid the occurrence of stem-like phenotype in cancer cells and it was found to diminish clonogenic activity, indicating decreased capacity for proliferation by tumour cells[46]. *In vitro* studies demonstrate 1632's ability to reduce tumour sphere formation, which correlates with reduced *in vivo* tumour formation and metastasis. Most importantly, 1632 does not appear to have instantaneous cytotoxic effects but rather selectively inhibit tumour-specific characteristics of cells[46].

Secondly, tristetraprolin (TTP) binds to the three prime untranslated region (3' UTR) of LIN28A mRNA that stimulates its decay. As a result, the increased mature *let-7* levels lead to suppression of *CDC34* expression, which prevents unregulated cell cycle progression to curb the growth of cancer cells. Furthermore, expression of TTP has an inverse correlation with LIN28A levels in ovarian adenocarcinoma and human cancer cell lines including breast adenocarcinoma, erythroleukaemia, HCC, and neuron-committed teratocarcinoma[47].

Thirdly, compounds such as TPEN inhibits LIN28A's ZKDs by chelating zinc ions to catalyse apoptosis in LIN28A-expressing stem cells while L171 directly binds to LIN28A's CSDs to disrupt RNA binding and LIN28A-mediated oligouridylation of let-7[48]. Studies demonstrated that TPEN targeted LIN28-expressing mouse ESCs but non-LIN28-expressing HeLa cells as well while L171 was effective in LIN28-dependent human leukaemia cells and ESCs. However, TPEN's zinc chelation is not specific to LIN28A so it could cause apoptosis in cells that do not express LIN28A and L171 has a low potency for its inhibitory effects so both compounds require improvements. Moreover, there have been other potential LIN28A inhibitors such as 5-(methylamino) nicotinic acid that could block LIN28-mediated oligouridylation and gossypol that is hypothesised to hinder growth of LIN28-expressing tumours by suppressing oncoproteins such as Bcl-1 and MSI1, but further research would need to be conducted into their mechanisms and efficacy[48].

LIN28A inhibitors such as C1632 can restore *let-7*–mediated downregulation of programmed death ligand-1 (PD-L1). PD-L1 is frequently overexpressed in cancer cells and is a mechanism through which these cells evade T-cell recognition of tumour-specific and enhance tumour progression. Furthermore, high expression levels of PD-L1 are associated with more malignant tumour subtypes and poor prognosis in patients. By restoring *let-7* levels, C1632 can hamper tumour growth by hindering proliferation of cancer cells and improve the immune surveillance[49]. Currently, C1632 treatment can suppress PD-L1 in antigen-presenting cells such as THP-1 macrophages, and elevate secretion of interferon gamma and tumour necrosis factor alpha to enhance their T-cell mediated anti-tumour activity[49].

In vitro studies involving treatment with C1632 did not seem to exhibit cytotoxic effects as significant increase in apoptosis was not observed. However, this does not necessarily translate to a therapeutically effective dose against cancer in humans. Interestingly, metformin and C1632 produce synergistic anti-tumour effects in oral squamous cell carcinoma (OSCC). Studies suggest that metformin activates Dicer *via* the AMP-activated protein kinase pathway to enable maturation of *let-7*. Consequently, a decline in proliferative and migratory capacity of human OSCC cells *in vitro* (reduced closure of wound) and decline in tumour growth *in vivo* (reduced weight), without obvious signs of toxicity were observed [50]. While this combined treatment is promising for a non-invasive treatment of OSCC, the side effects and immunoreactivity in humans are unclear so further testing is needed.

In addition, LIN28 expression has been positively correlated with aldehyde dehydrogenase (ALDH) levels, a marker of CSCs and particularly with a subpopulation of tumour cells that are ALDH 1 positive ($ALDH1^+$)[51]. ALDHs could affect mechanisms in DNA repair and radioresistance and thus, contribute to carcinogenesis. Since LIN28 regulates and maintains the $ALDH1^+$ cell population through the *let-7* pathway or a *let-7* independent pathway through reprogramming factors such as OCT4, inhibiting LIN28 would diminish the tumour cell population. This could be carried out by either manipulating TUTase to increase let-7 or using nanoparticle-delivered LIN28 small interfering RNA or let-7.

In fact, research has explored nanobodies that can directly interact with a functional region on the TUT4 known as 106-reside LIN28: Let-7 interaction (LLI) fragment. These nanobodies can bind to the LLI fragments to interfere with the recruitment of TUTase and impeding LIN28-dependent (*i.e.* involving TUT4) oligouridylation of pre-let-7 microRNAs and LIN28-independent monouridylation of group II pre-let-7 microRNAs[51]. Hence, inhibition of TUT4 activity leads to elevated levels of mature *let-7*; countering the potential oncogenic implications of the LIN28/*let-7* pathway.

Lastly, ubiquitin-specific protease 28 (USP28) is a deubiquitinase that removes polyubiquitin from proteins such as LIN28A to stop the proteasomal degradation, thereby stabilising and extending its half-life. Studies indicate that USP28 augments LIN28A's inhibitory and oncogenic function. The former function involves enhanced inhibition of let-7 while the latter function involves enhanced colony formation, cell migration and invasion, and cell anchorage-independent proliferation[52]. Moreover, USP28 is overexpressed in cancers such as colorectal cancer and non-small cell lung cancer. This can be attributed to USP28 stabilising proto-oncogenic factors such as MYC. Considering MYC can facilitate cancer cell proliferation, it is hypothesised that USP28 can influence the LIN28-mediated cancer cell proliferation as well[52]. Therefore, disrupting USP28 itself or targeting other proteins that regulate it could become a viable option for cancer therapy.

Neuropathies

In optical neuropathies, retinal ischaemia-reperfusion (RIR) injury is characterised by expedited neuronal cell death due to lack of nutrients and oxygen as well as reactive oxygen species (ROS). Treatment with rasagiline and idebenone can utilise LIN28A's inhibitory effects on caspase-3 to mitigate oxidative damage by ROS and apoptosis[53]. Next, these drugs can upregulate Dicer expression through the LIN28A/*let-7* pathway, which enables cleavage of pre-miRNA into mature miRNA for optic neuroprotection and retinal development. Therefore, this combined treatment can alleviate RIR injury[53].

In auditory neuropathies, sensorineural hearing loss can be due to loss of auditory neurons. *In vitro* studies demonstrated that LIN28 overexpression activates basic helix-loop-helix (bHLH) transcription factors *via let-7* inhibition and upregulates Sox2 and HMGA2, which leads to increased proliferation and reprogramming of inner ear glial cells into neurons[54]. Therefore, neuronal dedifferentiation and proliferation could possibly restore auditory function. These findings indicate the potential of LIN28A in cell replacement therapy.

CONCLUSION

Since its discovery, LIN28A has been found to regulate several physiological processes such as stem cell renewal and differentiation, tissue repair, and glucose metabolism through *let-7* dependent and independent pathways. While downstream signalling pathways such as the insulin-Akt-mTor pathway and certain mRNA targets such as HMGA2 have been identified, the exact mechanisms have not been completely understood. Next, it remains unclear how these pathways eventuate in different and sometimes, contrasting effects in cell types. Pathologically, overexpression of LIN28A is generally correlated with poor prognosis in certain cancers, and negative outcomes in some biliary diseases and neuropathies. Consequently, therapeutic approaches have been developed, which either target LIN28A or other proteins which interact with LIN28A. By inhibiting LIN28A expression or function and manipulating its pathways, cellular proliferation and differentiation, and tissue repair can be regulated, which would especially be imperative in cancer therapy and tissue regeneration. However, further research is required before the efficacy of these approaches can be verified.

ACKNOWLEDGEMENTS

I would like to thank Dr. Rajaraman Eri for his guidance in writing this review. I would also like to thank him and Tauseef Ahmad for providing constructive feedback.

FOOTNOTES

Author contributions: Wu K wrote the review; all authors have read and approved the final version of the review.

Conflict-of-interest statement: The authors declare no conflict of interest.

Country/Territory of origin: Australia

ORCID number: Kenneth Wu 0000-0002-1666-6152; Tauseef Ahmad 0000-0001-5322-9413; Rajaraman Eri 0000-0003-1688-8043.

S-Editor: Fan JR
L-Editor: A
P-Editor: Fan JR

REFERENCES

1 **Mayr F**, Heinemann U. Mechanisms of Lin28-mediated miRNA and mRNA regulation--a structural and functional perspective. *Int J Mol Sci* 2013; **14**: 16532-16553 [PMID: 23939427 DOI: 10.3390/ijms140816532]

2 **Tsialikas J**, Romer-Seibert J. LIN28: roles and regulation in development and beyond. *Development* 2015; **142**: 2397-2404 [PMID: 26199409 DOI: 10.1242/dev.117580]
3 **Shyh-Chang N**, Daley GQ. Lin28: primal regulator of growth and metabolism in stem cells. *Cell Stem Cell* 2013; **12**: 395-406 [PMID: 23561442 DOI: 10.1016/j.stem.2013.03.005]
4 **Amen AM**, Ruiz-Garzon CR, Shi J, Subramanian M, Pham DL, Meffert MK. A Rapid Induction Mechanism for Lin28a in Trophic Responses. *Mol Cell* 2017; **65**: 490-503.e7 [PMID: 28132840 DOI: 10.1016/j.molcel.2016.12.025]
5 **Ustianenko D**, Chiu HS, Treiber T, Weyn-Vanhentenryck SM, Treiber N, Meister G, Sumazin P, Zhang C. LIN28 Selectively Modulates a Subclass of Let-7 MicroRNAs. *Mol Cell* 2018; **71**: 271-283.e5 [PMID: 30029005 DOI: 10.1016/j.molcel.2018.06.029]
6 **Lee H**, Han S, Kwon CS, Lee D. Biogenesis and regulation of the let-7 miRNAs and their functional implications. *Protein Cell* 2016; **7**: 100-113 [PMID: 26399619 DOI: 10.1007/s13238-015-0212-y]
7 **Kim SK**, Lee H, Han K, Kim SC, Choi Y, Park SW, Bak G, Lee Y, Choi JK, Kim TK, Han YM, Lee D. SET7/9 methylation of the pluripotency factor LIN28A is a nucleolar localization mechanism that blocks let-7 biogenesis in human ESCs. *Cell Stem Cell* 2014; **15**: 735-749 [PMID: 25479749 DOI: 10.1016/j.stem.2014.10.016]
8 **Hafner M**, Max KE, Bandaru P, Morozov P, Gerstberger S, Brown M, Molina H, Tuschl T. Identification of mRNAs bound and regulated by human LIN28 proteins and molecular requirements for RNA recognition. *RNA* 2013; **19**: 613-626 [PMID: 23481595 DOI: 10.1261/rna.036491.112]
9 **Cho J**, Chang H, Kwon SC, Kim B, Kim Y, Choe J, Ha M, Kim YK, Kim VN. LIN28A is a suppressor of ER-associated translation in embryonic stem cells. *Cell* 2012; **151**: 765-777 [PMID: 23102813 DOI: 10.1016/j.cell.2012.10.019]
10 **Wilbert ML**, Huelga SC, Kapeli K, Stark TJ, Liang TY, Chen SX, Yan BY, Nathanson JL, Hutt KR, Lovci MT, Kazan H, Vu AQ, Massirer KB, Morris Q, Hoon S, Yeo GW. LIN28 binds messenger RNAs at GGAGA motifs and regulates splicing factor abundance. *Mol Cell* 2012; **48**: 195-206 [PMID: 22959275 DOI: 10.1016/j.molcel.2012.08.004]
11 **Qiu C**, Ma Y, Wang J, Peng S, Huang Y. Lin28-mediated post-transcriptional regulation of Oct4 expression in human embryonic stem cells. *Nucleic Acids Res* 2010; **38**: 1240-1248 [PMID: 19966271 DOI: 10.1093/nar/gkp1071]
12 **Li C**, Sako Y, Imai A, Nishiyama T, Thompson K, Kubo M, Hiwatashi Y, Kabeya Y, Karlson D, Wu SH, Ishikawa M, Murata T, Benfey PN, Sato Y, Tamada Y, Hasebe M. A Lin28 homologue reprograms differentiated cells to stem cells in the moss Physcomitrella patens. *Nat Commun* 2017; **8**: 14242 [PMID: 28128346 DOI: 10.1038/ncomms14242]
13 **Parisi S**, Passaro F, Russo L, Musto A, Navarra A, Romano S, Petrosino G, Russo T. Lin28 is induced in primed embryonic stem cells and regulates let-7-independent events. *FASEB J* 2017; **31**: 1046-1058 [PMID: 27920151 DOI: 10.1096/fj.201600848R]
14 **Seabrook JL**, Cantlon JD, Cooney AJ, McWhorter EE, Fromme BA, Bouma GJ, Anthony RV, Winger QA. Role of LIN28A in mouse and human trophoblast cell differentiation. *Biol Reprod* 2013; **89**: 95 [PMID: 24006280 DOI: 10.1095/biolreprod.113.109868]
15 **Yang M**, Yang SL, Herrlinger S, Liang C, Dzieciatkowska M, Hansen KC, Desai R, Nagy A, Niswander L, Moss EG, Chen JF. Lin28 promotes the proliferative capacity of neural progenitor cells in brain development. *Development* 2015; **142**: 1616-1627 [PMID: 25922525 DOI: 10.1242/dev.120543]
16 **Li N**, Zhong X, Lin X, Guo J, Zou L, Tanyi JL, Shao Z, Liang S, Wang LP, Hwang WT, Katsaros D, Montone K, Zhao X, Zhang L. Lin-28 homologue A (LIN28A) promotes cell cycle progression *via* regulation of cyclin-dependent kinase 2 (CDK2), cyclin D1 (CCND1), and cell division cycle 25 homolog A (CDC25A) expression in cancer. *J Biol Chem* 2012; **287**: 17386-17397 [PMID: 22467868 DOI: 10.1074/jbc.M111.321158]
17 **Shyh-Chang N**, Zhu H, Yvanka de Soysa T, Shinoda G, Seligson MT, Tsanov KM, Nguyen L, Asara JM, Cantley LC, Daley GQ. Lin28 enhances tissue repair by reprogramming cellular metabolism. *Cell* 2013; **155**: 778-792 [PMID: 24209617 DOI: 10.1016/j.cell.2013.09.059]
18 **Wang XW**, Li Q, Liu CM, Hall PA, Jiang JJ, Katchis CD, Kang S, Dong BC, Li S, Zhou FQ. Lin28 Signaling Supports Mammalian PNS and CNS Axon Regeneration. *Cell Rep* 2018; **24**: 2540-2552.e6 [PMID: 30184489 DOI: 10.1016/j.celrep.2018.07.105]
19 **Shinoda G**, Shyh-Chang N, Soysa TY, Zhu H, Seligson MT, Shah SP, Abo-Sido N, Yabuuchi A, Hagan JP, Gregory RI, Asara JM, Cantley LC, Moss EG, Daley GQ. Fetal deficiency of lin28 programs life-long aberrations in growth and glucose metabolism. *Stem Cells* 2013; **31**: 1563-1573 [PMID: 23666760 DOI: 10.1002/stem.1423]
20 **Zacharewicz E**, Lamon S, Russell AP. MicroRNAs in skeletal muscle and their regulation with exercise, ageing, and disease. *Front Physiol* 2013; **4**: 266 [PMID: 24137130 DOI: 10.3389/fphys.2013.00266]
21 **Corre C**, Shinoda G, Zhu H, Cousminer DL, Crossman C, Bellissimo C, Goldenberg A, Daley GQ, Palmert MR. Sex-specific regulation of weight and puberty by the Lin28/let-7 axis. *J Endocrinol* 2016; **228**: 179-191 [PMID: 26698568 DOI: 10.1530/JOE-15-0360]
22 **Docherty CK**, Salt IP, Mercer JR. Lin28A induces energetic switching to glycolytic metabolism in human embryonic kidney cells. *Stem Cell Res Ther* 2016; **7**: 78 [PMID: 27230676 DOI: 10.1186/s13287-016-0323-2]
23 **Kim JD**, Toda C, Ramírez CM, Fernández-Hernando C, Diano S. Hypothalamic Ventromedial Lin28a Enhances Glucose Metabolism in Diet-Induced Obesity. *Diabetes* 2017; **66**: 2102-2111 [PMID: 28550108 DOI: 10.2337/db16-1558]
24 **Balzeau J**, Menezes MR, Cao S, Hagan JP. The LIN28/let-7 Pathway in Cancer. *Front Genet* 2017; **8**: 31 [PMID: 28400788 DOI: 10.3389/fgene.2017.00031]
25 **Thornton JE**, Gregory RI. How does Lin28 let-7 control development and disease? *Trends Cell Biol* 2012; **22**: 474-482 [PMID: 22784697 DOI: 10.1016/j.tcb.2012.06.001]
26 **Roncarati R**, Lupini L, Shankaraiah RC, Negrini M. The Importance of microRNAs in RAS Oncogenic Activation in Human Cancer. *Front Oncol* 2019; **9**: 988 [PMID: 31612113 DOI: 10.3389/fonc.2019.00988]
27 **Ma X**, Li C, Sun L, Huang D, Li T, He X, Wu G, Yang Z, Zhong X, Song L, Gao P, Zhang H. Lin28/let-7 axis regulates aerobic glycolysis and cancer progression *via* PDK1. *Nat Commun* 2014; **5**: 5212 [PMID: 25301052 DOI: 10.1038/ncomms6212]
28 **Zhang Y**, Li C, Hu C, Wu Q, Cai Y, Xing S, Lu H, Wang L, Huang, Sun L, Li T, He X, Zhong X, Wang J, Gao P, Smith ZJ, Jia W, Zhang H. Lin28 enhances de novo fatty acid synthesis to promote cancer progression *via* SREBP-1. *EMBO Rep*

2019; **20**: e48115 [PMID: 31379107 DOI: 10.15252/embr.201948115]
29 **Wang T**, He Y, Zhu Y, Chen M, Weng M, Yang C, Zhang Y, Ning N, Zhao R, Yang W, Jin Y, Li J, Redpath RJ, Zhang L, Jin X, Zhong Z, Zhang F, Wei Y, Shen G, Wang D, Liu Y, Wang G, Li X. Comparison of the expression and function of Lin28A and Lin28B in colon cancer. *Oncotarget* 2016; **7**: 79605-79616 [PMID: 27793004 DOI: 10.18632/oncotarget.12869]
30 **Mizuno R**, Kawada K, Sakai Y. The Molecular Basis and Therapeutic Potential of *Let-7* MicroRNAs against Colorectal Cancer. *Can J Gastroenterol Hepatol* 2018; **2018**: 5769591 [PMID: 30018946 DOI: 10.1155/2018/5769591]
31 **Xiong H**, Zhao W, Wang J, Seifer BJ, Ye C, Chen Y, Jia Y, Chen C, Shen J, Wang L, Sui X, Zhou J. Oncogenic mechanisms of Lin28 in breast cancer: new functions and therapeutic opportunities. *Oncotarget* 2017; **8**: 25721-25735 [PMID: 28147339 DOI: 10.18632/oncotarget.14891]
32 **Shen B**, Yuan Y, Zhang Y, Yu S, Peng W, Huang X, Feng J. Long non-coding RNA FBXL19-AS1 plays oncogenic role in colorectal cancer by sponging miR-203. *Biochem Biophys Res Commun* 2017; **488**: 67-73 [PMID: 28479250 DOI: 10.1016/j.bbrc.2017.05.008]
33 **Zhang Y**, Xiao X, Zhou W, Hu J, Zhou D. LIN28A-stabilized FBXL19-AS1 promotes breast cancer migration, invasion and EMT by regulating WDR66. *In Vitro Cell Dev Biol Anim* 2019; **55**: 426-435 [PMID: 31140103 DOI: 10.1007/s11626-019-00361-4]
34 **King CE**, Wang L, Winograd R, Madison BB, Mongroo PS, Johnstone CN, Rustgi AK. LIN28B fosters colon cancer migration, invasion and transformation through let-7-dependent and -independent mechanisms. *Oncogene* 2011; **30**: 4185-4193 [PMID: 21625210 DOI: 10.1038/onc.2011.131]
35 **Liu Y**, Li H, Feng J, Cui X, Huang W, Li Y, Su F, Liu Q, Zhu J, Lv X, Chen J, Huang D, Yu F. Lin28 induces epithelial-to-mesenchymal transition and stemness *via* downregulation of let-7a in breast cancer cells. *PLoS One* 2013; **8**: e83083 [PMID: 24349438 DOI: 10.1371/journal.pone.0083083]
36 **Zhong Y**, Yang S, Wang W, Wei P, He S, Ma H, Yang J, Wang Q, Cao L, Xiong W, Zhou M, Li G, Shuai C, Peng S. The interaction of Lin28A/Rho associated coiled-coil containing protein kinase2 accelerates the malignancy of ovarian cancer. *Oncogene* 2019; **38**: 1381-1397 [PMID: 30266988 DOI: 10.1038/s41388-018-0512-9]
37 **Enriquez VA**, Cleys ER, Da Silveira JC, Spillman MA, Winger QA, Bouma GJ. High LIN28A Expressing Ovarian Cancer Cells Secrete Exosomes That Induce Invasion and Migration in HEK293 Cells. *Biomed Res Int* 2015; **2015**: 701390 [PMID: 26583126 DOI: 10.1155/2015/701390]
38 **Fang LL**, Wang XH, Sun BF, Zhang XD, Zhu XH, Yu ZJ, Luo H. Expression, regulation and mechanism of action of the miR-17-92 cluster in tumor cells (Review). *Int J Mol Med* 2017; **40**: 1624-1630 [PMID: 29039606 DOI: 10.3892/ijmm.2017.3164]
39 **Song H**, Xu W, Song J, Liang Y, Fu W, Zhu XC, Li C, Peng JS, Zheng JN. Overexpression of Lin28 inhibits the proliferation, migration and cell cycle progression and induces apoptosis of BGC-823 gastric cancer cells. *Oncol Rep* 2015; **33**: 997-1003 [PMID: 25515921 DOI: 10.3892/or.2014.3674]
40 **McDaniel K**, Hall C, Sato K, Lairmore T, Marzioni M, Glaser S, Meng F, Alpini G. Lin28 and let-7: roles and regulation in liver diseases. *Am J Physiol Gastrointest Liver Physiol* 2016; **310**: G757-G765 [PMID: 27012771 DOI: 10.1152/ajpgi.00080.2016]
41 **Nguyen LH**, Robinton DA, Seligson MT, Wu L, Li L, Rakheja D, Comerford SA, Ramezani S, Sun X, Parikh MS, Yang EH, Powers JT, Shinoda G, Shah SP, Hammer RE, Daley GQ, Zhu H. Lin28b is sufficient to drive liver cancer and necessary for its maintenance in murine models. *Cancer Cell* 2014; **26**: 248-261 [PMID: 25117712 DOI: 10.1016/j.ccr.2014.06.018]
42 **Yang H**, Li TW, Peng J, Tang X, Ko KS, Xia M, Aller MA. A mouse model of cholestasis-associated cholangiocarcinoma and transcription factors involved in progression. *Gastroenterology* 2011; **141**: 378-388, 388.e1 [PMID: 21440549 DOI: 10.1053/j.gastro.2011.03.044]
43 **Gori M**, Arciello M, Balsano C. MicroRNAs in nonalcoholic fatty liver disease: novel biomarkers and prognostic tools during the transition from steatosis to hepatocarcinoma. *Biomed Res Int* 2014; **2014**: 741465 [PMID: 24745023 DOI: 10.1155/2014/741465]
44 **Chang MY**, Oh B, Choi JE, Sulistio YA, Woo HJ, Jo A, Kim J, Kim EH, Kim SW, Hwang J, Park J, Song JJ, Kwon OC, Henry Kim H, Kim YH, Ko JY, Heo JY, Lee MJ, Lee M, Choi M, Chung SJ, Lee HS, Lee SH. LIN28A loss of function is associated with Parkinson's disease pathogenesis. *EMBO J* 2019; **38**: e101196 [PMID: 31750563 DOI: 10.15252/embj.2018101196]
45 **Kim JJ**, Savas JN, Miller MT, Hu X, Carromeu C, Lavallée-Adam M, Freitas BCG, Muotri AR, Yates JR 3rd, Ghosh A. Proteomic analyses reveal misregulation of LIN28 expression and delayed timing of glial differentiation in human iPS cells with MECP2 loss-of-function. *PLoS One* 2019; **14**: e0212553 [PMID: 30789962 DOI: 10.1371/journal.pone.0212553]
46 **Roos M**, Pradère U, Ngondo RP, Behera A, Allegrini S, Civenni G, Zagalak JA, Marchand JR, Menzi M, Towbin H, Scheuermann J, Neri D, Caflisch A, Catapano CV, Ciaudo C, Hall J. A Small-Molecule Inhibitor of Lin28. *ACS Chem Biol* 2016; **11**: 2773-2781 [PMID: 27548809 DOI: 10.1021/acschembio.6b00232]
47 **Kim CW**, Vo MT, Kim HK, Lee HH, Yoon NA, Lee BJ, Min YJ, Joo WD, Cha HJ, Park JW, Cho WJ. Ectopic over-expression of tristetraprolin in human cancer cells promotes biogenesis of let-7 by down-regulation of Lin28. *Nucleic Acids Res* 2012; **40**: 3856-3869 [PMID: 22210895 DOI: 10.1093/nar/gkr1302]
48 **Wang L**, Rowe RG, Jaimes A, Yu C, Nam Y, Pearson DS, Zhang J, Xie X, Marion W, Heffron GJ, Daley GQ, Sliz P. Small-Molecule Inhibitors Disrupt let-7 Oligouridylation and Release the Selective Blockade of let-7 Processing by LIN28. *Cell Rep* 2018; **23**: 3091-3101 [PMID: 29874593 DOI: 10.1016/j.celrep.2018.04.116]
49 **Yang X**, Lin X, Zhong X, Kaur S, Li N, Liang S, Lassus H, Wang L, Katsaros D, Montone K, Zhao X, Zhang Y, Bützow R, Coukos G, Zhang L. Double-negative feedback loop between reprogramming factor LIN28 and microRNA let-7 regulates aldehyde dehydrogenase 1-positive cancer stem cells. *Cancer Res* 2010; **70**: 9463-9472 [PMID: 21045151 DOI: 10.1158/0008-5472.CAN-10-2388]
50 **Yu C**, Wang L, Rowe RG, Han A, Ji W, McMahon C, Baier AS, Huang YC, Marion W, Pearson DS, Kruse AC, Daley GQ, Wu H, Sliz P. A nanobody targeting the LIN28:let-7 interaction fragment of TUT4 blocks uridylation of let-7. *Proc*

Natl Acad Sci U S A 2020; **117**: 4653-4663 [PMID: 32060122 DOI: 10.1073/pnas.1919409117]

51 **Chen Y**, Xie C, Zheng X, Nie X, Wang Z, Liu H, Zhao Y. LIN28/*let-7*/PD-L1 Pathway as a Target for Cancer Immunotherapy. *Cancer Immunol Res* 2019; **7**: 487-497 [PMID: 30651289 DOI: 10.1158/2326-6066.CIR-18-0331]

52 **Haq S**, Das S, Kim DH, Chandrasekaran AP, Hong SH, Kim KS, Ramakrishna S. The stability and oncogenic function of LIN28A are regulated by USP28. *Biochim Biophys Acta Mol Basis Dis* 2019; **1865**: 599-610 [PMID: 30543854 DOI: 10.1016/j.bbadis.2018.12.006]

53 **Lei D**, Shao Z, Zhou X, Yuan H. Synergistic neuroprotective effect of rasagiline and idebenone against retinal ischemia-reperfusion injury *via* the Lin28-let-7-Dicer pathway. *Oncotarget* 2018; **9**: 12137-12153 [PMID: 29552298 DOI: 10.18632/oncotarget.24343]

54 **Kempfle JS**, Luu NC, Petrillo M, Al-Asad R, Zhang A, Edge ASB. Lin28 reprograms inner ear glia to a neuronal fate. *Stem Cells* 2020; **38**: 890-903 [PMID: 32246510 DOI: 10.1002/stem.3181]

World Journal of Biological Chemistry

Submit a Manuscript: https://www.f6publishing.com

World J Biol Chem 2022 March 27; 13(2): 47-65

DOI: 10.4331/wjbc.v13.i2.47

ISSN 1949-8454 (online)

ORIGINAL ARTICLE

Basic Study

Mesenchymal stromal cell delivery as a potential therapeutic strategy against COVID-19: Promising evidence from *in vitro* results

Panagiotis Mallis, Theofanis Chatzistamatiou, Zetta Dimou, Eirini-Faidra Sarri, Eleni Georgiou, Maria Salagianni, Vasiliki Triantafyllia, Evangelos Andreakos, Catherine Stavropoulos-Giokas, Efstathios Michalopoulos

Specialty type: Cell biology

Provenance and peer review: Invited article; Externally peer reviewed.

Peer-review model: Single blind

Peer-review report's scientific quality classification

Grade A (Excellent): A
Grade B (Very good): B
Grade C (Good): 0
Grade D (Fair): D
Grade E (Poor): 0

P-Reviewer: Alberca RW, Brazil; Munteanu C, Romania; Zhang Z, China

Received: November 6, 2021
Peer-review started: November 6, 2021
First decision: December 27, 2021
Revised: December 28, 2021
Accepted: March 6, 2022
Article in press: March 6, 2022
Published online: March 27, 2022

Panagiotis Mallis, Theofanis Chatzistamatiou, Zetta Dimou, Eirini-Faidra Sarri, Eleni Georgiou, Catherine Stavropoulos-Giokas, Efstathios Michalopoulos, Hellenic Cord Blood Bank, Biomedical Research Foundation Academy of Athens, Athens 11527, Greece

Maria Salagianni, Vasiliki Triantafyllia, Evangelos Andreakos, Laboratory of Immunobiology, Center for Clinical, Experimental Surgery and Translational Research, Biomedical Research Foundation Academy of Athens, Athens 11527, Greece

Corresponding author: Panagiotis Mallis, MSc, PhD, Associate Research Scientist, Teaching Assistant, Hellenic Cord Blood Bank, Biomedical Research Foundation Academy of Athens, No. 4 Soranou Ephessiou Street, Athens 11527, Greece. pmallis@bioacademy.gr

Abstract

BACKGROUND

Severe acute respiratory syndrome coronavirus 2 (SARS-CoV-2) is responsible for the coronavirus disease 2019 (COVID-19) pandemic, which was initiated in December 2019. COVID-19 is characterized by a low mortality rate (< 6%); however, this percentage is higher in elderly people and patients with underlying disorders. COVID-19 is characterized by mild to severe outcomes. Currently, several therapeutic strategies are evaluated, such as the use of anti-viral drugs, prophylactic treatment, monoclonal antibodies, and vaccination. Advanced cellular therapies are also investigated, thus representing an additional therapeutic tool for clinicians. Mesenchymal stromal cells (MSCs), which are known for their immunoregulatory properties, may halt the induced cytokine release syndrome mediated by SARS-CoV-2, and can be considered as a potential stem cell therapy.

AIM

To evaluate the immunoregulatory properties of MSCs, upon stimulation with COVID-19 patient serum.

METHODS

MSCs derived from the human Wharton's Jelly (WJ) tissue and bone marrow (BM) were isolated, cryopreserved, expanded, and defined according to the criteria outlined by the International Society for Cellular Therapies. Then, WJ and

BM-MSCs were stimulated with a culture medium containing 15% COVID-19 patient serum, 1% penicillin-streptomycin, and 1% L-glutamine for 48 h. The quantification of interleukin (IL)-1 receptor a (Ra), IL-6, IL-10, IL-13, transforming growth factor (TGF)-β1, vascular endothelial growth factor (VEGF)-a, fibroblast growth factor (FGF), platelet-derived growth factor (PDGF), and indoleamine-2,3-dioxygenase (IDO) was performed using commercial ELISA kits. The expression of HLA-G1, G5, and G7 was evaluated in unstimulated and stimulated WJ and BM-MSCs. Finally, the interactions between MSCs and patients' macrophages were established using co-culture experiments.

RESULTS

Thawed WJ and BM-MSCs exhibited a spindle-shaped morphology, successfully differentiated to "osteocytes", "adipocytes", and "chondrocytes", and in flow cytometric analysis were characterized by positivity for CD73, CD90, and CD105 (> 95%) and negativity for CD34, CD45, and HLA-DR (< 2%). Moreover, stimulated WJ and BM-MSCs were characterized by increased cytoplasmic granulation, in comparison to unstimulated cells. The HLA-G isoforms (G1, G5, and G7) were successfully expressed by the unstimulated and stimulated WJ-MSCs. On the other hand, only weak expression of HLA-G1 was identified in BM-MSCs. Stimulated MSCs secreted high levels of IL-1Ra, IL-6, IL-10, IL-13, TGF-β1, FGF, VEGF, PDGF, and IDO in comparison to unstimulated cells ($P < 0.05$) after 12 and 24 h. Finally, macrophages derived from COVID-19 patients successfully adapted the M2 phenotype after co-culturing with stimulated WJ and BM-MSCs.

CONCLUSION

WJ and BM-MSCs successfully produced high levels of immunoregulatory agents, which may efficiently modulate the over-activated immune responses of critically ill COVID-19 patients.

Key Words: SARS-CoV-2; COVID-19; MSCs; Stem cell therapy; Cytokine storm; Immunomodulation

Core Tip: Coronavirus disease 2019 (COVID-19) is responsible for the acute respiratory distress syndrome occurrence, a disorder that might prove life-threatening for a great number of hospitalized patients. As an alternative to the already evaluated therapeutic protocols, mesenchymal stromal cells (MSCs) can be evaluated as a potential stem cell therapy. MSCs exert key immunoregulatory properties, either through direct or indirect contact. In the current study, stimulated Wharton's Jelly and bone marrow-MSCs produced high levels of anti-inflammatory cytokines and growth factors and also efficiently performed the M2 phenotype switch of macrophages. Considering this data, MSCs could be considered as a valuable stem cell therapy for better COVID-19 management.

Citation: Mallis P, Chatzistamatiou T, Dimou Z, Sarri EF, Georgiou E, Salagianni M, Triantafyllia V, Andreakos E, Stavropoulos-Giokas C, Michalopoulos E. Mesenchymal stromal cell delivery as a potential therapeutic strategy against COVID-19: Promising evidence from *in vitro* results. *World J Biol Chem* 2022; 13(2): 47-65
URL: https://www.wjgnet.com/1949-8454/full/v13/i2/47.htm
DOI: https://dx.doi.org/10.4331/wjbc.v13.i2.47

INTRODUCTION

Coronavirus disease 2019 (COVID-19), which is caused by severe acute respiratory syndrome coronavirus 2 (SARS-CoV-2), was initially reported in Wuhan, China in 2019[1-3]. Currently, it is believed that the zoonotic transmission of SARS-CoV-2 initiated from a local wild animal market in Wuhan. Due to the fast global transmission of SARS-CoV-2, the World Health Organization (WHO) declared on January 2020 the COVID-19 as a Public Health Emergency of International Concern (PHEIC), followed by an upgrade to pandemic status on March 11 of the same year[4,5].

Now, COVID-19 represents a major global issue, counting more than 281484620 total cases and more than 5409113 fatalities, since the initial outbreak[6]. Indeed, the COVID-19 pandemic has spread in more than 220 countries[6,7]. Accurate date regarding the worldwide spread of COVID-19 can be provided by global monitoring platforms such as Johns Hopkins University Coronavirus Research Center[6].

SARS-CoV-2 affects primarily the respiratory system (upper and lower respiratory tract), followed by infection of multiple organs (*e.g.*, the liver, kidney, intestine, and heart)[8]. The clinical manifestations of SARS-CoV-2 include: (1) Initial mild symptoms, such as cough, fever, fatigue, and general malaise; (2)

moderate symptoms, such as pneumonia and low oxygen levels; and (3) severe symptoms, including the acute respiratory distress syndrome, cytokine release syndrome, and multiorgan failure[8,9]. COVID-19 is currently characterized by an average mortality rate of less than 6% globally; however, in patients aged above 65 years old or patients with significant underlying disorders, the mortality rate is increasing dramatically[6,10,11]. Currently, it has been reported that the transmission of SARS-CoV-2 between healthy individuals can be performed through three main ways: (1) Contact transmission with SARS-CoV-2 positive subjects; (2) droplet; and (3) aerosol transmission. The latter might explain the fast transmission of SARS-CoV-2 globally[12].

The entry of SARS-CoV-2 to the host cells is mediated through the connection between the spike (S) protein and the angiotensin-converting enzyme (ACE) II receptor[8-12]. A second receptor named transmembrane protease serine 2 (TMPRSS2) favors the priming of the S protein and is implicated in the viral entry process[8-12]. After its entrance, SARS-CoV-2 is starting to multiply its virion to infect more cells. In this case, the host's immune system may recognize the SARS-CoV-2[8-12]. This can result in the local release of interferons, activation of immune cells (such as macrophages, dendritic cells [DCs], natural killer [NK] cells, and T and B lymphocytes), and finally virus clearance[8-12]. However, in case of escaping from the immune surveillance and recognition mechanisms, SARS-CoV-2 can induce severe pneumonia[13]. SARS-CoV-2 pathophysiology is related to the alveolar epithelial cell damage, which could result in ground-glass opacity of the lungs[14]. The latter is mediated mainly by the stimulated T helper (Th) 1, 2, and Th17 cells[13]. Critically ill patients are characterized by increased levels of several cytokines including IL-2, IL-6, IL-7, G-CSF, IP10, MCP1, MIP1A, and TNF-α, a situation which is also known as "cytokine storm"[13,15]. These patients are characterized by lymphopenia, thrombocytopenia, NK cell reduction, respiratory failure, and multi-organ injury (*e.g.*, cardiac and lung fibrosis)[16].

To date, several therapeutic strategies, which can ameliorate the above manifestations, have been proposed and used in the clinical setting[17]. Among them, antimalarial drugs such as hydroxychloroquine or chloroquine, doxycycline, corticosteroids, monoclonal antibodies against IL-6, and convalescent plasma antibodies have been applied in COVID-19 patients with different effectiveness results[17,18]. In this way, the prevention of SARS-CoV-2 transmission through the vaccination program may represent the best option against this pandemic. However, there are still a great number of patients that are hospitalized or require the intensive care unit, accompanied by connection to extracorporeal membrane oxygenation.

Considering the great prevalence of COVID-19, more therapeutic strategies targeting the aberrant host immune responses must be evaluated. One such therapeutic intervention with potential benefit for critically ill patients may be the utilization of mesenchymal stromal cells (MSCs)[19,20].

MSCs are non-hematopoietic stem cells with great immunoregulatory/immunosuppressive abilities. MSCs represent a mesodermal multipotent stem cell population, which initially was discovered in bone marrow (BM) aspirate samples by Bianco *et al*[21]. Currently, MSCs can be obtained from various sources of the human body, including the liver, lungs, adipose tissue (AT), umbilical cord blood, placenta, and umbilical cord tissue (Wharton's Jelly [WJ] tissue)[22]. Based on the proposed guidelines of the MSC Committee of the International Society for Cell and Gene Therapy (ISCT), MSCs must fulfill specific criteria[23,24]. Briefly, MSCs must exhibit: (1) Plastic-adhesion ability (spindle-shaped cells); (2) tri-lineage differentiation towards "osteocytes", "chondrocytes", and "adipocytes" under defined conditions; and (3) specific immunophenotype[23,24]. Interestingly, MSCs are characterized by positive and negative expression of specific cell surface markers (clusters of differentiation [CDs]). More than 95% of MSCs express CD73 (5'-nucleotidase), CD90 (Thy-1 antigen), and CD105 (endoglin), and < 2% express CD34 (hemopoietic stem cell marker), CD45 (pan-lymphocyte antigen), HLA-DR (HLA class II molecules), CD11b (macrophage marker), and CD19 (B-lymphocyte marker)[23,24].

Also, MSCs are considered as immune-evasive stem cells and thus cannot be recognized by the immune cells, *e.g.*, macrophages and T and B cells[25,26]. Intriguingly, the immune evasion of MSCs is elicited mainly by the lack of HLA class II molecules and costimulatory molecules such as CD80, CD86, CD40, and CD40 ligand[25,26].

Besides, according to the proposed guidelines by the ISCT, MSCs from different sources are characterized by variable functional properties. Indeed, fetal MSCs (*e.g.*, derived from amniotic fluid, placenta, and WJ tissue) may have significant differences in terms of proliferation and differentiation efficiency, telomere length, and telomerase activity, compared to adult MSCs (*e.g.*, adipose tissue and bone marrow)[22,27-29]. Also, it has been shown that fetal MSCs are characterized by better immunoregulatory/immunosuppressive properties and have acquired less mutagenic or epigenetic changes to their genome, in comparison to MSCs derived from adult sources[22,27-29].

MSCs are known for their immunoregulatory properties, mediated either through the cell-cell contact mechanisms or through the secretion of bioactive molecules[30]. MSCs have broad effects on the cells of innate and adaptive immunity. Specifically, MSCs can orchestrate the phenotype switching from proinflammatory M1 to anti-inflammatory M2 macrophages, promote the production of tolerogenic DCs, and induce T and B cell inhibition[31]. These functions can be mediated either through direct contact of MSCs with the immune cells and activation of cell signaling pathways (promoted after cell contact interactions) such as Fas/Fas ligand, TNF-α/TNF-R, PD-L1/PD-1, and HLA-G, or through the release of specific molecules, *e.g.*, indoleamine-2.3-dioxygenase (IDO), nitric oxide (NO), galectins, and the soluble forms of HLA-G (HLA-G5-G7)[31]. Currently, MSCs have been utilized in over 80 clinical

trials for COVID-19, registered to the international database clinicaltrials.gov (www. clinicaltrials.gov) [32,33]. In the majority of the studies, the safety and efficiency of the infused MSCs have been well evaluated[32-37]. However, in those studies, the exact interplay between MSCs and hyper-stimulated immune cells in COVID-19 patients has not been satisfactorily explained.

Furthermore, due to the mesodermal lineage differentiation capacity of MSCs, these cells may exert beneficial tissue regeneration of the damaged tissue. The pathogenesis of COVID-19 involves the injury of the alveolar epithelium, which further may induce lung fibrosis, a state which is known as ground glass opacity. MSCs can either be differentiated to endothelial and epithelial cells or can direct the differentiation of epithelial and endothelial progenitor cells, through a paracrine manner. MSCs can exert both immunoregulatory properties and tissue regeneration abilities, and therefore, their use as an alternative therapeutic strategy in critically-ill COVID-19 patients must be strongly considered by the physicians.

Therefore, the aim of the current study was focused on the *in vitro* evaluation of the immunoregulatory properties of MSCs, upon stimulation with serum obtained from critically ill COVID-19 patients. COVID-19 patient serum is characterized by high levels of pro-inflammatory cytokines, which can stimulate efficiently the MSCs under *in vitro* conditions. This assessment was performed in cryopreserved MSCs derived from WJ and BM samples. In this way, the discrepancy in the key immunoregulatory properties between WJ and BM-MSCs may be revealed. The obtained data may give fundamental insights into the beneficial effects of MSCs in tolerating the overactivated immune responses. Furthermore, the MSCs from both sources may be proven to be a satisfactory cell therapy, ameliorating the manifestations of COVID-19.

MATERIALS AND METHODS

Isolation, expansion, and cryopreservation of WJ-MSCs

WJ-MSCs were isolated from the human umbilical cords (hUCs) that were delivered to Hellenic Cord Blood Bank (HCBB). In the current study, hUCs (n = 10) derived from full-term (gestational ages 38-40 wk) normal and caesarian deliveries, were used for the isolation of the WJ-MSCs. All hUCs were accompanied by informed consent, which was in accordance with the declaration of Helsinki and conformed with the ethical standards of the Greek National Ethical Committee. The informed consent was provided by the mothers, few days before the delivery. The overall study has received approval from the Institution's ethical board (Reference No. 1754, January 21, 2021). After the delivery of the hUCs to the HCBB, the samples were processed immediately for MSCs isolation. Initially, the hUCs were rinsed in excess 1 × phosphate buffer saline (PBS, Sigma-Aldrich, Darmstadt, Germany), to remove any blood clots. Then, isolation of WJ tissue was performed with the use of sterile instruments. The isolated WJ tissue was dissected into small pieces (0.3 cm × 0.3 cm) and placed in a 6-well culture plate (Costar, Corning Life, Canton, MA, United States). Finally, 1 mL of complete culture medium was added to each well, and the cultures were transferred to an incubator at 37 °C in an atmosphere containing 5% CO_2, for a time period of 18 d. After 18 d of cultivation, the cultures were microscopically checked and in case of cell confluency near to 80% (in each well), the MSCs were trypsinized (Trypsin-EDTA solution 0.25% w/v, Gibco, Thermo Fisher Scientific, Waltham, United States) and placed to a 75 cm^2 tissue culture flask. The WJ-MSCs were grown in the cell cultures until reaching passage (P) 3. Then, WJ-MSCs at P3 were detached from the flasks and centrifuged at 500 g for 6 min, and the cell pellet was cryopreserved using the Bambanker solution (Nippon Genetics, Duren, Germany) into 1.8 mL cryotubes. Finally, the cryotubes were placed into a Mr. Frosty freezing container (Thermo Fisher Scientific), ensuring the control rate freezing (1 °C/min) of the cells. The cryotubes were transferred to a liquid nitrogen tank at -196 °C for a time period of 6 mo.

The complete culture medium used in the whole study consisted of α-minimum essentials medium (α -MEM, Sigma-Aldrich) supplemented with 15% fetal bovine serum (FBS, Sigma-Aldrich), 1% v/v penicillin-streptomycin (P-S, Sigma Aldrich), and 1% v/v L-glutamine (L-Glu, Sigma Aldrich).

Isolation, expansion and cryopreservation of BM-MSCs

BM-MSCs (n = 10) were isolated from donor samples, after obtaining the signed informed consent for the current study. BM-MSCs were isolated accordingly. Ten milliliters of BM was transferred to 75 cm^2 tissue cultured flasks supplemented with the complete culture medium. The BM cell cultures were placed in an incubator at 37 °C in an atmosphere containing 5% CO_2 for a time period of 10 d. BM-MSCs were microscopically checked for their morphology and confluency, followed by passaging to 175 cm^2 tissue culture flasks. The BM-MSCs were grown in the cell cultures until reaching P3. Then cryopreservation of BM-MSCs was performed (in the same way as mentioned above). Finally, the cryotubes remained in the liquid nitrogen tank for a time period of 6 mo.

Thawing procedure of WJ and BM-MSCs

The thawing procedure of MSCs from both sources involved their quick transfer from -196 °C to a water bath at 37 °C (Memmert, Germany). Then, thawed MSCs of each cryotube were transferred to 50 mL

conical falcon tubes (Costar, Corning Life) with the addition of 30 mL 1 × PBS (Sigma-Aldrich), followed by centrifugation at 500 g for 6 min. Finally, the MSCs were placed to 75 cm^2 cell culture flasks (Costar, Corning Life) with 14 mL of complete culture medium, and remained until further processing.

Characterization of WJ and BM-MSCs

Following the criteria of the ISCT, the WJ and BM-MSCs were evaluated for their quality characteristics. The quality check of the WJ and BM-MSCs at P3 involved: (1) Microscopic examination; (2) evaluation of differentiation capacity into "osteocytes", "adipocytes", and "chondrocytes"; and (3) flow cytometry analysis for the evaluation of specific CDs expression.

Morphological assessment of WJ and BM-MSCs was performed using an inverted light microscope (Leica DM L2, Leica, Microsystems, Weltzar, Germany) and images were acquired with IC Imaging Control (The ImagineSource, Bremen, Germany) and processed with Image J (v1.533, National Institute of Health, United States).

The ability of MSCs from both sources to differentiate to "osteocytes", "adipocytes", and "chondrocytes" was evaluated. For this purpose, the StemPro Osteogenesis, Adipogenesis, and Chondrogenesis kits (Thermo Fischer Scientific) were used, according to the manufacturer's instructions. To validate their successful differentiation, histological analysis with the use of specific stains was performed. Alizarin Red S, Oil Red O, and Alcian Blue (Sigma-Aldrich) were applied for the evaluation of calcium deposition, lipid droplet, and glycosaminoglycans (sGAGs) production, respectively.

Determination of the MSCs' immunophenotype was performed using a panel of 15 monoclonal antibodies, using the FACS Calibur (BD Biosciences, Franklin Lakes, NJ, United States). Specifically, fluorescein (FITC) labeled antibodies against CD90, CD45, CD29, CD31, and HLA-ABC, phycoerythrin (PE) labeled antibodies against CD44, CD3, CD11b, and CD34, peridinin-chlorophyll-protein (PerCP) labeled antibodies against CD105 and HLA-DR, and allophycocyanin (APC) labeled antibodies against CD73, CD10, and CD340 were used. All monoclonal antibodies were purchased from Becton Dickinson (BD biosciences). For each tube, on average 10000 total events were acquired. Complete flow cytometric analysis was performed with FlowJo v10 (BD biosciences).

Stimulation of WJ and BM-MSCs with COVID-19 patient serum

Stimulation of WJ-MSCs (n = 10) and BM-MSCs (n = 10) was achieved using a culture medium supplemented with COVID-19 patient serum (COVID-19 culture medium) obtained from five critically ill patients. These critically ill patients (n = 5) exhibited moderate to severe symptoms and had pneumonia which was confirmed by radiological findings. The COVID-19 patients fulfilled the following criteria: (1) Respiratory distress (≥ 30 breaths/min); (2) low oxygen levels (≤ 93% at rest); and (3) arterial partial pressure of oxygen (PaO_2)/fraction of inspired oxygen (FiO_2) ≤ 300 mmHg with no other organ failure. All patients were acquired from the 2nd Respiratory Clinic of "Sotiria" General Chest Diseases Hospital, Athens, Greece. All patients were informed and provided informed consent for the current study.

Thawed WJ and BM-MSCs at a density of 150 × 10^3 cells/well were placed in 6-well plates with 1 mL of COVID-19 culture medium and incubated for a time period of 48 h. Then, removal of the culture medium was performed, followed by extensive washes with 1 × PBS. Finally, α-MEM (Sigma-Aldrich) supplemented with 1% v/v P-S (Sigma-Aldrich) was added and remained until cytokine and growth factor quantification analysis was performed. COVID-19 medium consisted of α-MEM (Sigma-Aldrich) supplemented with 15% v/v COVID-19 patient serum and 1% v/v P-S (Sigma-Aldrich).

Characterization of stimulated MSCs

Stimulated MSCs from both sources were evaluated for their morphological features. For this purpose, stimulated MSCs were observed using an inverted light microscope (Leica DM L2, Microsystems), and images were acquired with IC Imaging Control (The Imagine Source) and processed with Image J (v1.533, National Institute of Health, United States). Furthermore, cell viability and number were measured in unstimulated and stimulated MSCs. To perform this evaluation, cell counting and viability estimation were performed using trypan blue dye. The measurement was performed in the automated Cell Countess system (Thermo Fischer Scientific).

Immunophenotype evaluation was also performed in MSCs before and after the stimulation with COVID-19 patient serum. Immunophenotype analysis was performed using an antibody panel consisting of antibodies against CD73, CD90, CD105, CD29, CD340, CD45, and HLA-DR. The whole process was performed as described in the previous section (Characterization of WJ and BM-MSCs).

Cytokine and growth factor quantification analysis

The cytokine and growth factor profile of stimulated WJ and BM MSCs was performed using ELISA. Specifically, IL-1 receptor antagonist (RA), IL-6, IL-10, and IL-13 and transforming growth factor (TGF)-β1, vascular endothelial growth factor (VEGF), fibroblast growth factor (FGF)-1, platelet-derived growth factor (PDGF), and IDO were evaluated in unstimulated and stimulated MSCs. The quantification of cytokines and growth factors was performed after 12 and 24 h (after the addition of α-MEM with 1% v/v P-S, Sigma-Aldrich). All assays were performed according to the manufacturer's instructions and

the final concentration was estimated through interpolation to the standard curve.

Evaluation of HLA-G mRNA expression in stimulated MSCs

Evaluation of the HLA-G expression was performed in unstimulated (n = 3) and stimulated MSCs derived either from the WJ (n = 3) or BM (n = 3). Briefly, the mRNA from the aforementioned MSCs was isolated using the TRI reagent (Sigma-Aldrich) following the manufacturer's instructions. Then, the mRNA was quantified and 800 ng was used for the performance of reverse transcription (RT)-polymerase chain reaction (PCR). Complementary DNA (cDNA) was used as a template and amplified using the primers listed in Table 1. The PCR was performed on Eppendorf Master Cycler (Eppendorf, Hamburg, Germany), involving the following steps: (1) Initial denaturation at 95 °C for 15 s; (2) denaturation at 94 °C for 30 s; (3) annealing at 60–61 °C for 90s; and (4) extension at 72 °C for 3 min. The current program involved a total of 35 cycles. The PCR products were analyzed by 1% v/v agarose gel electrophoresis (Biorad, California, United States). Glyceraldehyde 3-phosphate dehydrogenase (GAPDH) was used as an internal housekeeping gene for the evaluation of the results.

Evaluation of HLA-G protein expression

Evaluation of HLA-G expression was performed using the flow cytometric and immunofluorescence assays. The indirect immunofluorescence assay was performed in unstimulated MSCs (n = 3/from each source) and stimulated WJ (n = 3) and BM-MSCs (n = 3). MSCs were placed at a density of 2 × 10^4 on culture slides (Costar, Corning Life). When confluency was observed, the cells were exposed to 10% v/v neutral formalin (Sigma-Aldrich) for 20 min and fixed. Initially, antigen epitope retrieval was applied in all samples, followed by blocking and addition of primary monoclonal antibody against human HLA-G (1:1000, Catalog MA1-10359, Thermo Fisher Scientific). Extensive washes were performed and the secondary FITC-conjugated mouse IgG antibody (1:100, Sigma-Aldrich) was added. DAPI (Thermo Fisher Scientific) was used to stain nuclei. The slides were mounted and observed under a fluorescence microscope. Images were acquired with LEICA SP5 II microscope equipped with LAS Suite v2 software (Leica, Microsystems).

Isolation of peripheral blood mononuclear cells and macrophage differentiation

The isolation of human peripheral blood mononuclear cells (PBMCs) was performed from critically ill COVID-19 patients (n = 5). Specifically, 10 mL of peripheral blood was diluted (1:1) with 1 × PBS (Sigma-Aldrich) and placed carefully on the top of Ficoll (Sigma-Aldrich). Then, centrifugation was performed at 450 g for 30 min. PBMCs layer was isolated and placed in a different conical tube, where 10 mL of 1 × PBS (Sigma-Aldrich) was added. Then, centrifugation at 350 g for 5 min was performed. Finally, the CD14+ cells were separated with negative selection using the human CD14+ cell enrichment (Stem Cell Technologies) according to the manufacturer's instructions.

The isolated monocytes were submitted to macrophage differentiation. Monocytes at a density of 1 × 10^5/well were added to 24-transwell (bottom) plates with 1 mL of α-MEM supplemented with 1% v/v L-Glu, 1% v/v P-S, and 100 ng/ ml granulocyte-macrophage colony-stimulating factor (GM-CSF). The differentiation process lasted 9 d, and the medium was changed twice a week.

Co-culture of stimulated MSCs with macrophages

After macrophage differentiation from the patient's PBMCs, co-culturing experiments with the stimulated WJ (n = 5) and BM-MSCs (n = 5) were performed. This set of experiments was performed using 24 trans-well plates (Costar, Corning Life) coupled with 3 μm pores. Unstimulated (n = 5) and stimulated WJ (n = 5) or BM-MSCs (n = 5) at a density of 5 × 10^4/well were placed on the top, while patient's macrophages were placed on the bottom of the trans-well plates. Finally, 1 mL of regular culture medium was added to each well, and the trans-wells placed were transferred to an incubator at 37 °C in an atmosphere containing 5% CO_2 for 10 d. The change of the medium was performed once a week. The cultures were observed under an inverted light microscope (Leica DM L2, Microsystems). The images were acquired with IC Imaging Control (The ImagineSource) and processed with Image J (v1.533, National Institute of Health, United States). Also, flow cytometry analysis, to determine the macrophage phenotype switch from M1 to M2, was performed using the markers CD14-PE, CD45-FITC, CD11b-PE, CD29-FITC, and CD163-PerCP. All monoclonal antibodies were purchased from Becton Dickinson (BD biosciences). For each tube, on average 10000 total events were acquired. Complete flow cytometric analysis was performed with FlowJo v10 (BD biosciences).

Statistical analysis

Statistical analyses were performed using the statistical software GraphPad Prism v 6.01 (GraphPad Software, San Diego, CA, United States). All comparisons in the current study were performed by the unpaired non-parametric Kruskal–Wallis test. Statistically significant difference between group values was considered when the P value was less than 0.05. Values are presented as the mean ± SD.

Table 1 Primer sequences used in the current study

Gene	Forward	Reverse	Size
HLA-G1	AGGAGACACGGAACACCAAG	CCAGCAACGATACCCATGAT	685
HLA-G5	AACCCTCTTCCTGCTGCTCT	GCCTCCATCTCCCTCCTTAC	895
HLA-G7	AACCCTCTTCCTGCTGCTCT	TTACTCACTGGCCTCGCTCT	331
GAPDH	AAGGGCCCTGACAACTCTTT	CTCCCCTCTTCAAGGGGTCT	244

RESULTS

Evaluation of WJ and BM-MSCs characteristics

Prior to stimulation of cells with the culture medium containing COVID-19 patient serum, thawed WJ and BM-MSCs were comprehensively evaluated for their characteristics. MSCs from both sources were characterized as plastic adherent spindle-shaped cells with a few cytoplasmic vacuoles (Figure 1A and Supplementary Figure 1). Successful differentiation of MSCs to "osteocytes", "adipocytes", and "chondrocytes" was confirmed using specific histological stains. Specifically, Alizarin red S and oil red O stained positively the calcium deposits and oil-droplets, produced from WJ and BM-MSCs, respectively. Further characterization of MSCs involved the immunophenotypic evaluation, using the flow cytometry analysis. WJ and BM-MSCs shared similar size features (Figure 1B and C). On the other hand, BM-MSCs were characterized by increased cytoplasmic granulation and therefore greater forward to side scatter ratio, compared to WJ-MSCs (Figure 1B). Over 95% of both WJ and BM-MSCs expressed the CD73, CD90, CD105, CD10, CD29, and CD340, while less than 2% expressed CD34, CD45, HLA-DR, CD11b, and CD31(Figure 1C and Supplementary Table 1). The only discrepancy in CDs expression between WJ and BM-MSCs was found in HLA-ABC. Specifically, over 75% of WJ-MSCs expressed the HLA-ABC, while over 90%of BM-MSCs expressed the same marker (Figure 1C and Supplementary Table 1). Thawed MSCs from both sources retained successfully their morphological and immunophenotypic characteristics until reaching P4, and hence can be considered as well-defined MSCs, which can efficiently be used in the current study.

Evaluation of stimulated WJ and BM-MSCs characteristics

After the initial evaluation of WJ and BM-MSCs characteristics, stimulation with patient-derived COVID-19 serum was performed. WJ and BM-MSCs were exposed to culture medium containing COVID-19 patient serum for 48 h, followed by morphological, immunophenotypic, and molecular evaluations (Figure 2A). Morphological analysis using an inverted light microscope showed the preservation of the fibroblastic-like morphology of stimulated MSCs from both sources. Moreover, stimulated WJ and BM-MSCs exhibited increased cytoplasmic granulation, compared to unstimulated MSCs (Figure 2B). After 48 h of incubation with COVID-19 culture medium, the total cell number of stimulated WJ and BM-MSCs was $4.8 \pm 0.4 \times 10^5$ and $3.5 \pm 0.2 \times 10^5$, respectively (Supplementary Table 2). The initial cell number of WJ and BM-MSCs was $3.1 \pm 0.1 \times 10^5$ (for both cell sources). A statistically significant difference was found in cell numbers between unstimulated and stimulated WJ and BM-MSCs ($P < 0.001$, Supplementary Table 2). The viability rate of unstimulated WJ and BM-MSCs was 94 ± 1% and 93 ± 2%, respectively, while stimulated MSCs presented similar viability rates (Figure 2C). Further characterization of stimulated MSCs involved the immunophenotypic analysis. Stimulated WJ and BM-MSCs exhibited increased cytoplasmic granulation, thus confirming further the initial morphological evaluation (Figure 2D). No statistically significant alteration in CD expression was observed between stimulated and unstimulated WJ and BM-MSCs. Specifically, in unstimulated and stimulated MSCs obtained from both sources, > 95% of the cells expressed CD73, CD90, CD105, CD29, and CD340, while < 2% expressed CD45 and HLA-DR (Figure 2D). A detailed description of the CD marker expression in unstimulated and stimulated WJ and BM MSCs is provided as supplementary data (Supplementary Table 3).

Additional analysis involved the evaluation of the HLA-G expression in stimulated MSCs. For this purpose, RNA was isolated from unstimulated and stimulated MSCs, followed by the performance of RT-PCR and PCR. Finally, the PCR products were analyzed by agarose gel electrophoresis. In this study, the HLA-G1, G5, and G7 isoforms were determined. WJ-MSCs successfully expressed the HLA-G isoforms. Specifically, unstimulated WJ MSCs expressed the cytoplasmic HLA-G1 and the soluble forms of HLA-G5 and HLA-G7 (Figure 2E). Stimulated WJ-MSCs were characterized by elevated expression of the above HLA-G isoforms. On the contrary, BM-MSCs (unstimulated and stimulated) expressed only the HLA-G1 (Figure 2E). These results were further confirmed by indirect immunofluorescence. Stimulated WJ-MSCs exhibited higher expression of the HLA-G1 compared to the unstimulated cells (Figure 2F). On the other hand, BM-MSCs exhibited a weak fluorescence signal regarding the HLA-G1 (Figure 3F).

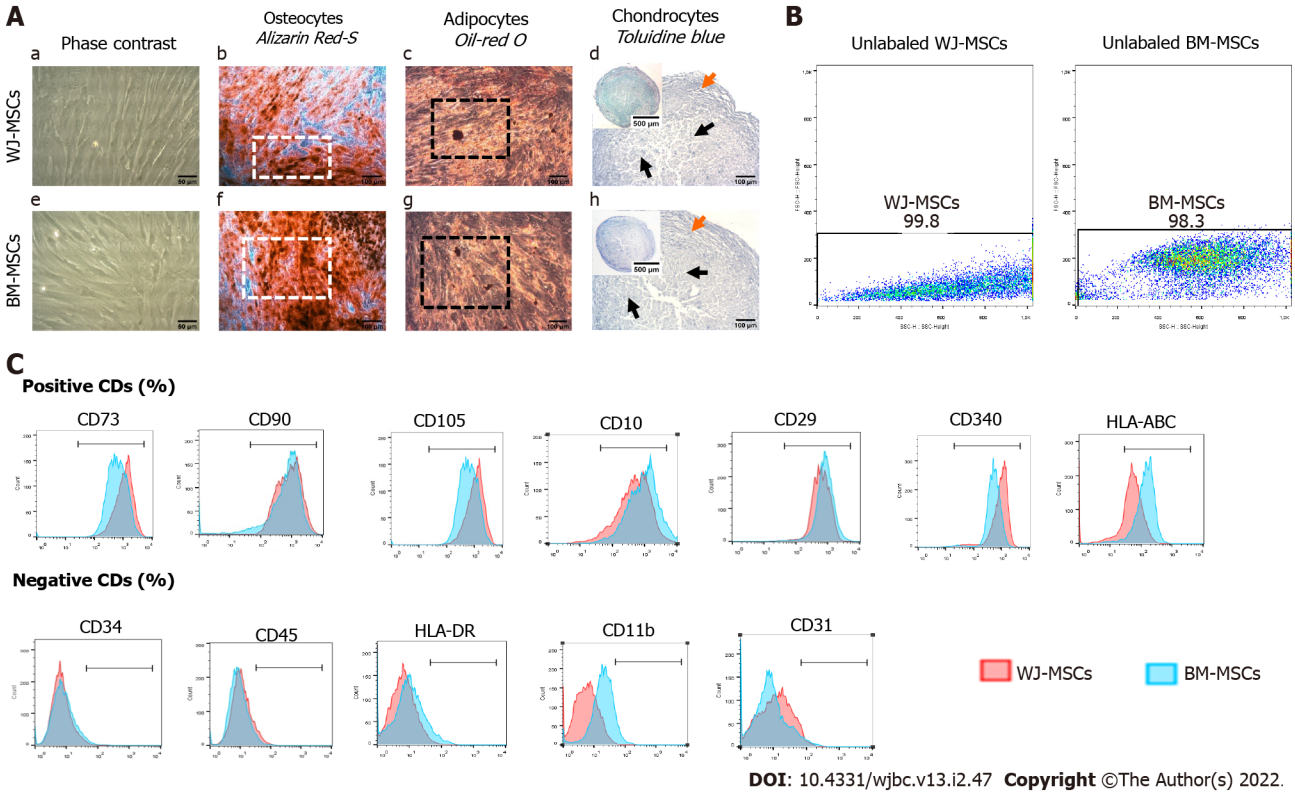

DOI: 10.4331/wjbc.v13.i2.47

Figure 1 Evaluation of characteristics of Wharton's Jelly and bone marrow-mesenchymal stromal cells. A: Morphological characteristics of mesenchymal stromal cells (MSCs) derived from Wharton's Jelly (WJ) tissue and bone marrow (BM). MSCs from both sources were characterized as spindle-shaped cells with a few internal vacuoles. Both WJ and BM-MSCs were successfully differentiated to "osteocytes", "adipocytes", and "chondrocytes". White squares and black squares indicate the presence of calcium deposits and oil droplets, respectively. Black and orange arrows indicate the differentiated and undifferentiated state, respectively. a and e: Original magnification 20 ×, scale bars = 50 μm; b-d and f-h: Original magnification 10 ×, scale bars = 100 μm; B: Unlabeled WJ and BM-MSCs; C: Evaluation of CD marker expression by WJ and BM-MSCs. BM: Bone marrow; MSCs: Mesenchymal stromal cells; WJ: Wharton's Jelly.

Quantification of cytokines and growth factors

The next step of the current study involved the examination of the effect of inflammatory stimuli on the release of the immunosuppressive cytokines and growth factors by the WJ and BM-MSCs. Stimulated MSCs from both sources were evaluated for the cytokine secretion including IL-1Ra, IL-6, IL-10, and IL-13, growth factor production including TGF-b1, FGF, VEGF, and PDGF, and the release of the immunosuppressive agent IDO. The secretion of the aforementioned factors was evaluated after 12 and 24 h, from the initial activation of MSCs with COVID-19 culture medium. The results of this study indicated an increase in the release of the immunoregulatory agents compared to the unstimulated cells after 12 and 24 h (Figure 3). Specifically, after 8 h from the initial activation, the levels of IL-1RA, IL-6, IL-10, and IL-13 were 924 ± 100, 66 ± 11, 195 ± 51, and 174 ± 23 pg/mL for the stimulated WJ-MSCs, respectively, and 432 ± 162, 33 ± 16, 88 ± 24, and 132 ± 24 pg/mL for the stimulated BM-MSCs, respectively (Figure 3A-D, Supplementary Table 4). After 24 h, the levels of the same cytokines were 407 ± 57, 44 ± 7, 103 ± 14, and 114 ± 5 pg/mL for the stimulated WJ-MSCs, respectively, and 235 ± 50, 21 ± 4, 71 ± 8, and 79 ± 14 pg/mL for the stimulated BM-MSCs, respectively (Figure 4A-D, Supplementary Table 5). Statistically significant differences were found in cytokine release after 12 and 24 h between stimulated and unstimulated MSCs ($P < 0.05$) and also between stimulated WJ and BM-MSCs ($P < 0.05$). In the same way, the levels of TGF-b1, FGF, VEGFA, and PDGF after 8h of activation for the stimulated WJ-MSCs were 955 ± 210, 1048 ± 82, 801 ± 143 and 941 ± 107 pg/mL, respectively, and for stimulated BM-MSCs were 840 ± 43, 995 ± 88, 790 ± 108, and 826 ± 145 pg/mL, respectively (Figure 3E-H, Supplementary Table 4). After 24 h, the levels of the above growth factors for the stimulated WJ-MSCs were 813 ± 140, 669 ± 84, 646 ± 102, and 754 ± 74 pg/mL, respectively, and for the stimulated BM-MSCs were 653 ± 182, 627± 107, 585 ± 55, and 672 ± 108 pg/mL, respectively (Figure 4E-H, Supplementary Table 5). Finally, the levels of the immunosuppressive agent IDO after 12 and 24 h from the initial activation for the activated WJ-MSCs were 1228 ± 92 and 835 ± 77 pg/mL and for stimulated BM-MSCs were 1152 ± 80 and 674 ± 100 pg/mL, respectively (Figures 3I and 4I, Supplementary Tables 4 and 5). A detailed description regarding the levels of all immunomodulatory agents derived from unstimulated and stimulated WJ and BM-MSCs is provided in Table S4.

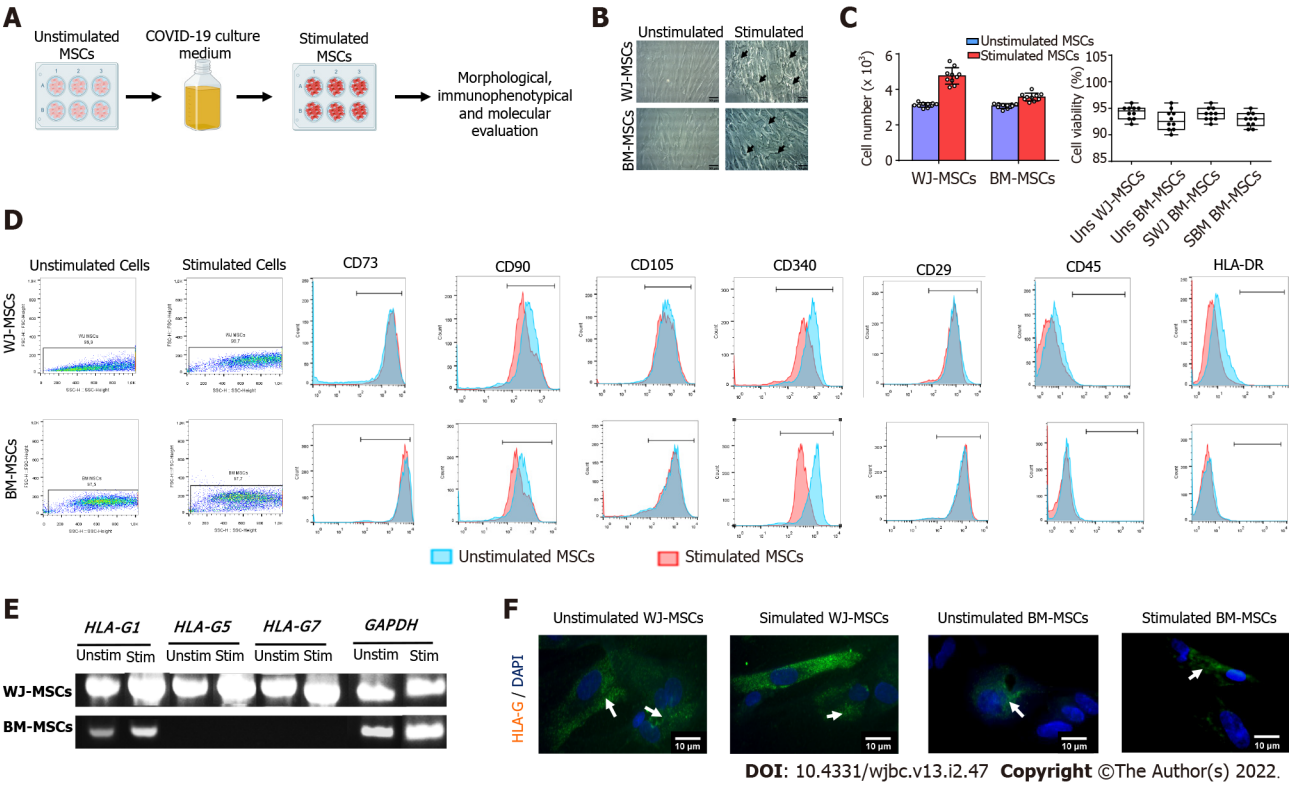

DOI: 10.4331/wjbc.v13.i2.47

Figure 2 Comprehensive characterization of characteristics of stimulated Wharton's Jelly and bone marrow mesenchymal stromal cells.
A: Experimental workflow; B: Morphological analysis of characteristics of unstimulated and stimulated Wharton's Jelly (WJ) and bone marrow-mesenchymal stromal cells (BM-MSCs). Original magnification 20 ×, scale bars = 50 μm; C: Determination of cell proliferation and viability. Statistically significant differences were observed in cell proliferation between stimulated and unstimulated WJ-MSCs ($P < 0.05$) and stimulated and unstimulated BM-MSCs ($P < 0.05$). No statistically significant difference was observed in cell viability either in an unstimulated or stimulated state ($P = 0.873$); D: Immunophenotypic analysis of stimulated and unstimulated WJ and BM-MSCs. Over 95% of WJ and BM-MSCs in both states expressed CD73, CD90, CD105, CD29, and CD340, and less than 2% expressed CD34 and CD45; E: Determination of HLA-G isoforms (HLA-G1, G5, and G7) in unstimulated and stimulated MSCs from both sources; F: Indirect immunofluorescence against HLA-G1 in combination with DAPI stain was performed on unstimulated and stimulated WJ and BM-MSCs. Original magnification 63 ×, scale bars = 10 μm. BM: Bone marrow; MSCs: Mesenchymal stromal cells; WJ: Wharton's Jelly.

Evaluation of macrophage polarization

To investigate the ability of WJ and BM-MSCs in inducing an anti-inflammatory phenotype in macrophages obtained from COVID-19 patients, co-culturing experiments were performed. Briefly, the isolated CD14+ monocytes from PBMCs were induced to differentiate into M1 macrophages in the presence of GM-CSF. Over 90% of differentiated cells expressed CD11b in flow cytometry analysis, a typical macrophage marker. Then, stimulated WJ and BM-MSCs were added to the top of the transwell plates, while the differentiated macrophages were placed in the bottom of the plate. Initially, macrophages were characterized by a round-shape morphology, which is a typical feature of the M1 phenotype. After 9 d of co-culturing, shapeshift of macrophages was observed with the use of an inverted light microscope (Figure 5). Specifically, macrophages exhibited a spindle-shaped morphology, a common characteristic of the M2 phenotype. In addition, flow cytometry analysis showed an increase in the integrin b1 subunit (CD29) and the scavenger receptor (CD163) expression in macrophages after 9 d of co-culturing either with WJ or BM-MSCs (Supplementary Table 6). Statistically significant differences regarding the CD29 and CD163 were observed in macrophages before and after the co-culturing with the MSCs ($P < 0.001$). The above data indicated the positive effect of stimulated MSCs in macrophage polarization into the anti-inflammatory M2 phenotype.

DISCUSSION

The pandemic COVID-19, which was initiated at the end of 2019, has been considered a severe life-threatening condition[1-5]. COVID-19 now is a global public and economic burden for most countries[1-5]. SARS-CoV-2 is responsible for the severe acute respiratory distress syndrome occurrence, which may further cause lung fibrosis, multiorgan failure, and eventually life loss. The pathophysiologic mechanisms of SARS-CoV-2 include also the induction of CRS, which is associated with increased levels of IL-2, IL-6, IL-7, G-CSF, IP10, MCP1, MIP1A, and TNF-α[13-15]. CRS is also related to altered host

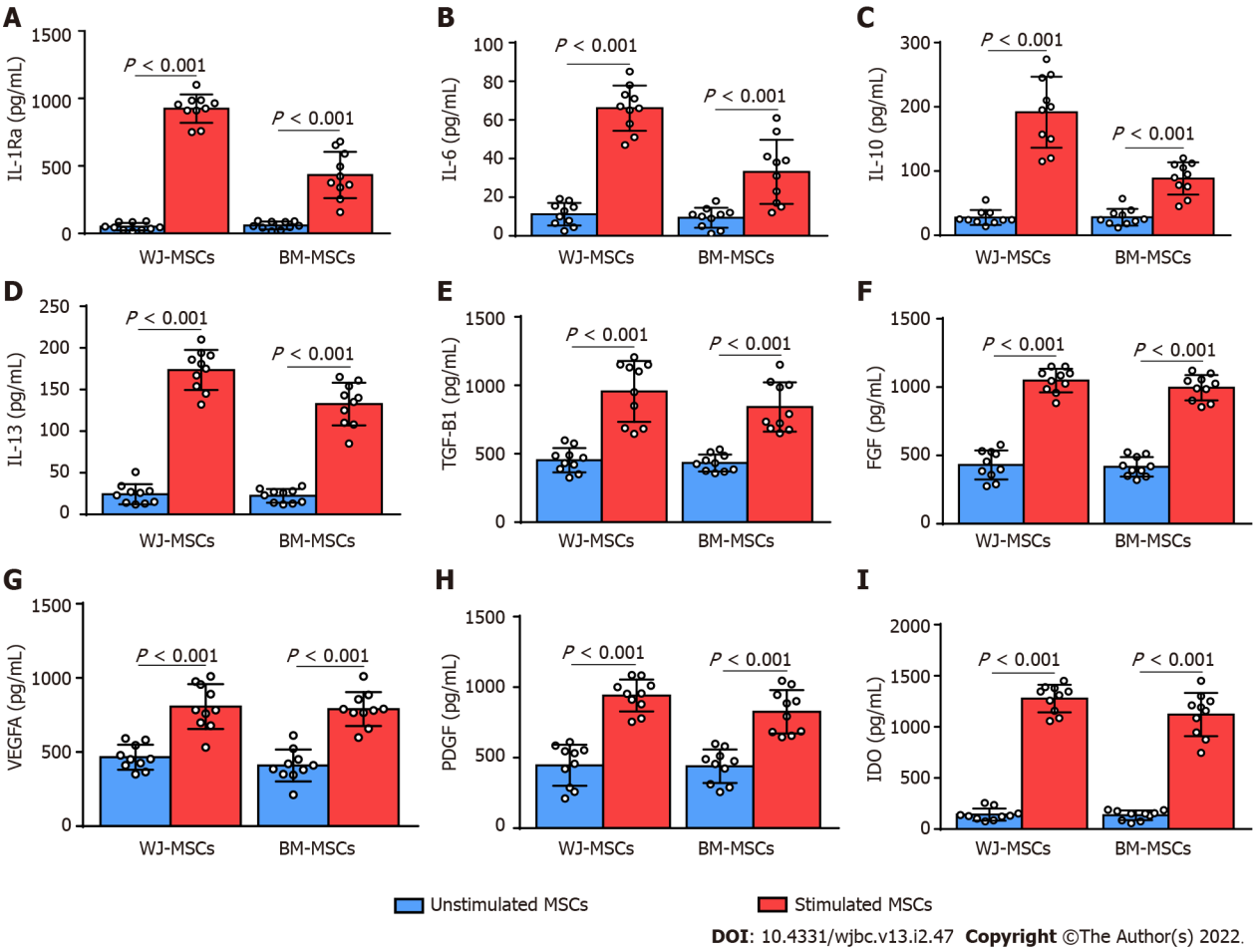

DOI: 10.4331/wjbc.v13.i2.47

Figure 3 Quantification of immunosuppressive agents after 12 h from the initial activation with coronavirus disease 2019 patient serum.
A-D: Quantification of cytokines including IL-1Ra, IL-6, IL-10, and IL-13 in unstimulated and stimulated Wharton's Jelly (WJ) and bone marrow-mesenchymal stromal cells (BM-MSCs); E-H: Quantification of growth factors including TGF-b1, FGF, VEGFA, and PDGF in unstimulated and stimulated WJ and BM-MSCs; I: Quantification of indoleamine-2,3-dioxygenase in unstimulated and stimulated WJ and BM-MSCs. BM: Bone marrow; MSCs: Mesenchymal stromal cells; WJ: Wharton's Jelly.

immune responses, and activation mostly of M1 macrophages, Th1, and Th17 cells. Until now, several therapeutic protocols have been evaluated, including the administration of antivirals drugs (such as remdesivir and favipiravir), corticosteroids, and monoclonal antibodies against IL-6, with the vaccination to emerge as the most promising solution[17,18]. However, besides the vaccination, modern cell therapies are now evaluated and considered as promising strategies for critically ill COVID-19 patients. In this way, MSCs, which are sharing key immunoregulatory properties, may serve as a potential stem cell therapy[25-32]. Currently, a great number of clinical trials (where the MSCs are used) are being performed, with very encouraging results[33-37]. However, until now, the studies focusing on the molecular mechanisms by which MSCs may exert their beneficial properties against COVID-19 are limited. Therefore, in the current study, we evaluated the immunoregulatory properties of stimulated WJ and BM-MSCs as a result stimulation with COVID-19 patient serum.

Initially, the characterization of the thawed WJ and BM-MSCs was performed, and no discrepancies were observed according to the already published literature[22-24]. Both thawed WJ and BM-MSCs fulfilled the criteria outlined by the ISCT and hence were considered as well-defined cells[23,24]. Then, stimulation of MSCs from both sources using COVID-19 patient serum was performed. Stimulated MSCs retained their initial morphology; however, increased cytoplasmic granulation was observed in the stimulated cells. Besides that, no alteration was observed in MSCs markers. Importantly, no variability in CD340 expression was observed between unstimulated and stimulated MSCs (from both sources). CD340 is a stem cell marker, and its preservation after the stimulation indicated no alteration in the stemness properties of MSCs[38]. Indeed, Kim *et al*[39] showed that increased levels of CD340 were associated with MSCs that can exert high stem cell characteristics and therapeutic benefits. Moreover, in the study of Kim *et al*[39], CD340+ MSCs highly expressed OCT4 and NANOG, accompanied by elevated growth ability and differentiation potential. Specifically, CD340+ MSCs exhibited increased differentiation capacity towards the "osteogenic" lineage, as it was also confirmed by the increased alkaline phosphatase signal intensity[39]. Moreover, in our study, it was shown that CD340+ WJ and BM-MSCs, besides the differentiation potential, were efficiently stimulated and

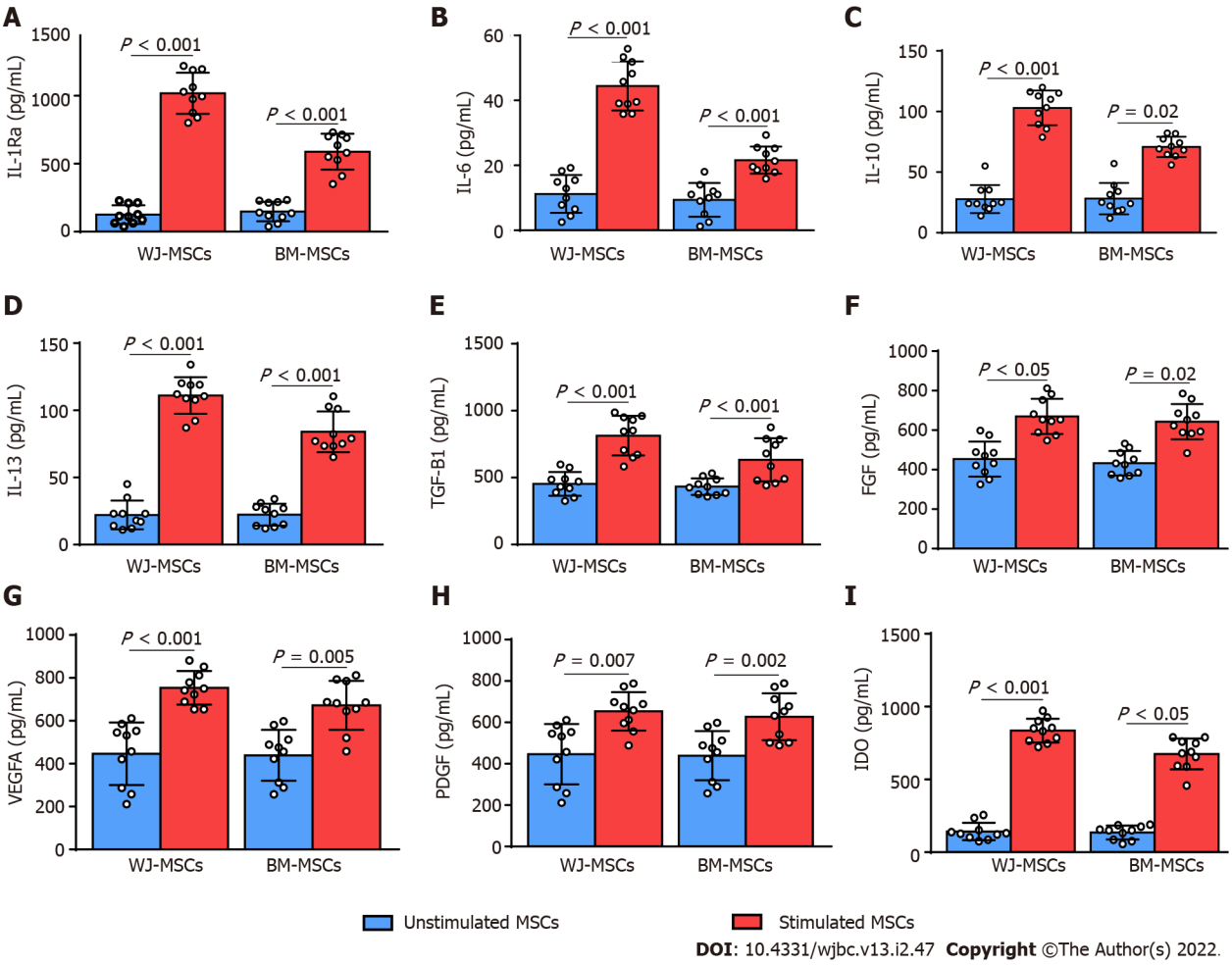

DOI: 10.4331/wjbc.v13.i2.47

Figure 4 Quantification of immunosuppressive agents after 24 h from the initial activation with coronavirus disease 2019 patient serum.
A-D: Quantification of cytokines including IL-1Ra, IL-6, IL-10, and IL-13 in unstimulated and stimulated Wharton's Jelly (WJ) and bone marrow mesenchymal stromal cells (BM-MSCs); E-H: Quantification of growth factors including TGF-b1, FGF, VEGFA, and PDGF in unstimulated and stimulated WJ and BM-MSCs; I: Quantification of IDO in unstimulated and stimulated WJ and BM-MSCs. BM: Bone marrow; MSCs: Mesenchymal stromal cells; WJ: Wharton's Jelly.

secreted a high amount of immunomodulatory agents.

Initially, the expression of the immunomodulatory molecule HLA-G was evaluated. Specifically, unstimulated and stimulated WJ-MSCs expressed the HLA-G1, HLA-G5, and HLA-G7 whereas only weak expression of HLA-G1 was found in BM-MSCs. HLA-G shares a close relationship with the extraembryonic tissues, where can induce the mother's tolerance against the semi-allogeneic fetus[40]. Considering this, it may explain the elevated levels of HLA-G expression in WJ-MSCs compared to BM-MSCs. WJ-MSCs are derived from the umbilical cord, an extraembryonic tissue, which is characterized by high HLA-G expression levels. Moreover, Yen *et al*[41] showed that adult MSCs (such as BM-MSCs) are characterized by different methylation patterns in the promoter region of the *HLA-G*, compared to MSCs from fetal tissues. Importantly, it was shown that different methylation patterns were also evident within the *HLA-G* gene between different MSCs sources[41]. Accordingly, the difference in methylation patterns might also explain the variability of HLA-G expression between the WJ and BM-MSCs. In the literature, controversial data regarding the expression of the HLA-G between MSCs from fetal and adult sources have also been reported[42-46]. It is well known that HLA-G shares important immunomodulatory properties, which can efficiently modulate the immune responses exerted by stimulated immune cells such as macrophages, DCs, NK cells, and T and B cells[31]. In this way, HLA-G might have a significant role in tolerating the CRS in critically ill COVID-19 patients.

Furthermore, priming of MSCs with COVID-19 patient serum enhanced both the secreted immunoregulatory and regenerative agents in response to the inflammatory stimuli. In the current study, it was observed that the COVID-19 inflammatory stimuli were able to increase the production of IL-1Ra, IL-6, IL-10, and IL-13 by WJ and BM-MSCs. It has been shown in the past that the secreted anti-inflammatory cytokines may act positively in the inflamed microenvironment, tolerating the over-activated immune responses[47-49]. Specifically, IL-1Ra which binds selectively to the secreted IL-1 can efficiently block the immune cell activation through downregulation of signaling pathways such as the nuclear factor kappa-light-chain-enhancer (NF-κB) of the stimulated B cells[50,51]. Importantly, several studies have shown that IL-1Ra and IL-10 have a synergistic effect in modulating the immune responses[52]. IL-10

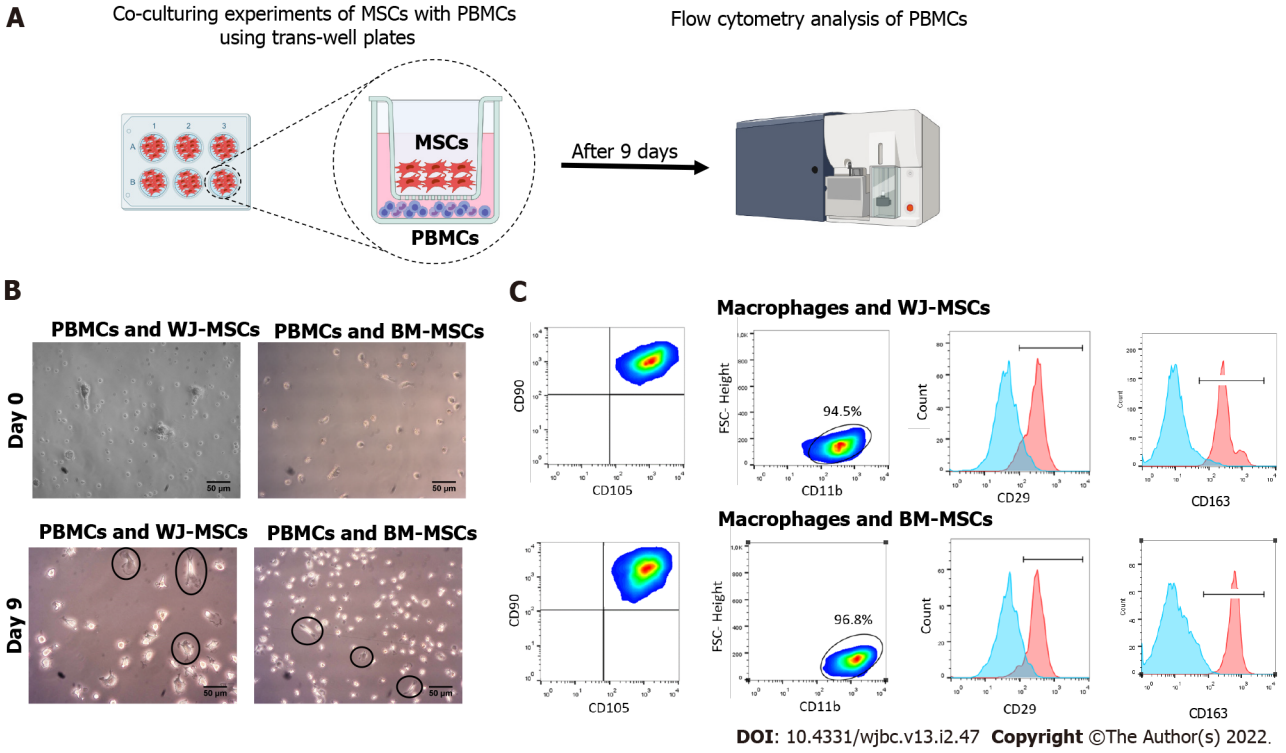

Figure 5 Co-culturing experiments of M1 macrophages with stimulated Wharton's Jelly and bone marrow-mesenchymal stromal cells. A: Schematic representation of the experimental workflow; B: Macrophage morphology was changed 9 d after co-culture either with Wharton's Jelly or bone marrow-mesenchymal stromal cells. After 9 d, macrophages exhibited a more elongated shape and plastic adherence. Black arrows indicate the presence of elongated plastic adherent cells; C: Flow cytometry analysis showed the positive expression of CD45, CD14, and CD11b by the differentiated macrophages. After 9 d, the macrophages exhibited an increase in the CD29 and CD163 expression, compared to the cells at day 0. Statistically significant differences regarding the CD29 and CD163 were observed in M2 compared to M1 macrophages ($P < 0.001$). BM: Bone marrow; MSCs: Mesenchymal stromal cells; WJ: Wharton's Jelly; PBMCs: Peripheral blood mononuclear cells.

can suppress the stimulated cellular population of innate and adaptive immunity such as the activated macrophages, inhibit the Th1 and promote the Th2 response, and also can act as an antagonist of IL-1 and TNF-a[52,53]. In the same way, IL-13 can cause a shift towards the Th2 response. Indeed, upon IL-13 binding to its receptor, activation of JAK-STAT1/STAT6 and IRS-1/IRS-2 pathways is induced, which further leads to the adaptation of Th2 response[54,55]. IL-13 is a known anti-inflammatory cytokine, which is also implicated in M2 phenotype switch and acts as an antagonist of IL-1β, IL-3, IL-12, and TNF-α[56-58]. In addition, COVID-19 stimulated MSCs secreted high levels of IL-6. IL-6 is a pleiotropic cytokine produced in the initial stages of inflammation, and exerts key functions in immune cells[58,59]. Critically ill COVID-19 patients have increased IL-6 levels, which is considered as the main mediator for the orchestration of the pro-inflammatory cytokines to the infected region[60]. However, there are several studies indicating that IL-6 can serve as a regulator between pro- and anti-inflammatory responses[61,62]. IL-6 can stimulate IL-10 production, which synergistically can act on activated immune cells[61-63]. Specifically, both cytokines can suppress the antigen presentation function of the activated DCs, thus resulting in the formation of the tolerogenic DCs[61-63]. Recently, Dorronsoro *et al* [64] showed that silencing of IL-6 with shRNA significantly induced impaired immunoregulatory functions by human MSCs. Therefore, IL-6 seems to play a significant role in the immunomodulation mediated by the activated MSCs[64]. The anti-inflammatory actions of the aforementioned cytokines can be enhanced by other immunosuppressive agents such as the secreted IDO. IDO is a strong immunoregulatory molecule that is implicated in the T cell cycle, by inhibiting the tryptophan catabolism to kynurenine[65]. In this way, T cells can be poised to G1 arrest state, thus their proliferation is stopped [66,67]. Besides T cells, IDO can exhibit an immunosuppressive action on B and NK cells, while its production is elevated by IFN-γ stimulated MSCs[31].

In addition, several growth factors are produced by the MSCs in response to the COVID-19 inflammatory stimuli. Among them, TGF-β, FGF, VEGF, and PDGF play a crucial role in the regulation of various fundamental immune functions, such as cell stimulation, migration, proliferation, and apoptosis [31]. Notably, the suppression of CD4+ and CD8+ T cell proliferation is induced through the upregulation of cyclin-dependent kinase (CDK) inhibitors p15, p21, and p27 and downregulation of c-Myc, cyclin D2, and E, a process which can be regulated by the secreted growth factors[68]. T cell suppression is mediated through the TGF-β/SMAD3-dependent downregulation of CDK4, as has been proposed by several research teams[69,70]. Secreted growth factors in combination with the anti-inflammatory

cytokines besides the described immunomodulation, can induce the proliferation of progenitor cells, favoring the tissue regeneration of the damaged tissue[71,72].

The immunoregulatory properties of the stimulated MSCs were further verified by the co-culture experiments. Differentiated macrophages derived from COVID-19 patients successfully adapted the anti-inflammatory M2 phenotype after their interaction with the stimulated MSCs. It has been proposed in the past that MSCs can educate and tolerate the inflammatory macrophages[73,74]. In the current study, we noticed the elevated expression of CD29 and CD163. Of note, CD163 represents a specific marker of the M2 phenotype[75,76]. CD29 represents the β1 integrin subunit, which is also related to the fibroblastic shape of the M2 macrophages[77,78]. M2 macrophage phenotype is closely related to the expression of anti-inflammatory properties, thus contributing both to immunomodulation and tissue regeneration. The results of this study were in agreement with the study of Domenis *et al*[79], showing the successful M2 phenotype switch after exosome (derived from MSCs) mediated crosstalk. In addition, de Witte *et al*[80] and Weiss *et al*[81] have shown that infused MSCs may follow the apoptotic or necroptotic program, thus undergoing phagocytosis by the alveolar macrophages. Through this process, the macrophages shift to the M2 phenotype efficiently.

MSCs currently are considered as Advanced Therapeutic Medicinal Products (ATMPs), hence clinical trials establishing the safe and tolerability of these cells must be conducted[20,32-37]. In the majority of the clinical trials, allogeneic or autologous MSCs are intravenously (IV) administrated in COVID-19 patients. Possible adverse events (AEs) that are associated with the IV administration include fever risk, toxicity, infection, pulmonary embolism, and possible malignancy formation. However, in the currently conducted clinical trials utilizing the MSCs as a possible COVID-19 treatment strategy, only an increased risk of fever was reported. Furthermore, after IV administration of MSCs, the AEs are considered mild to moderate. Besides the aforementioned AEs, other incidences also have been reported and evaluated for the possible relation with MSCs administration. The study of Shi *et al*[82] reported an increase in lactic acid dehydrogenase, serum alanine aminotransferase, creatine phosphatase, aspartate aminotransferase, and uric acid, and reported hypokalemia during the 1-year follow-up. However, all these AEs were on-site judged and considered as unrelated to the MSCs administration[82]. Considering these data, MSCs are a safe and tolerable therapy, therefore more clinical trials (phases I, II, and III) have been registered (www.clinicaltrials.gov) and are currently performed to further evaluate the potential application of these cells in critically ill COVID-19 patients.

At this point, it is worthy to mention the limitations of the current study. This study involved an initial evaluation of immunomodulatory agent release in a small sample size of WJ and BM-MSCs. Further evaluation of the immunomodulatory agents in a greater number of samples must be performed to verify better our initial results. Future experiments should also involve the evaluation of the direct interaction between MSCs and immune cells. Also, further assessment of the beneficial properties of MSCs may include their utilization in humanized ACE2 transgenic mouse models.

The results of this study represent only preliminary evidence; however, in this study, significant data which may decipher the molecular mechanisms associated with the immunomodulatory activity of MSCs have been presented. Besides the immunomodulatory properties, MSCs possess key differentiation capabilities, committed mostly to mesodermal lineage cell types. In this way, MSCs can act in both the immune regulation of the overactivated immune responses and alveolar epithelium regeneration. The latter may be related with the rapid reversal of ground-glass opacity in the lung, which consists of a major underlying disorder in critically ill COVID-19 patients. Additionally, in this study, it was shown that MSC therapy can be quickly administrated to COVID-19 patients, upon demand. Therefore, allogeneic MSCs can be isolated, expanded at great numbers, and cryopreserved over a long time. Upon IV administration to patients, MSCs can be activated by the microenvironment stimuli, therefore no need for initial *in vitro* priming is required.

MSCs should be considered as a safe alternative therapeutic option, which may improve the COVID-19 patients' condition and result in less loss of life.

CONCLUSION

In conclusion, MSCs derived either from the WJ or BM, can exert key immunoregulatory functions towards inflammation. SARS-CoV-2 have a broad effect in patients' body, orchestrating the production of the pro-inflammatory cytokines and also inducing extensive damage to alveolar epithelial cells[83]. MSCs are currently used in a great number of clinical trials, ameliorating efficiently the immune system dysregulation[32-37]. Importantly, MSCs from the BM are characterized by lower production of the studied immunoregulatory agents compared to WJ-MSCs. However, more research is required to characterize better the immunoregulation mediated by MSCs from various tissue sources. WJ-MSCs possess more naïve cells compared to MSCs derived from adult sources. Moreover, it has been shown that MSCs derived from fetal tissues are characterized by fewer mutations and epigenetic modifications, greater proliferation, and differentiation capacity, compared to adult MSCs[22] In addition, MSCs from fetal tissues can be isolated noninvasively (compared to adult MSCs)[22]. Allogeneic MSCs are considered immune-evasive cells, as they are not expressing either the HLA-DR or stimulatory (CD40)

and co-stimulatory molecules (CD80 and CD86)[22,26]. Therefore, their infusion in human subjects should be considered safe. Furthermore, Avanzini *et al*[84] showed that MSCs are negative for ACE2 and TMPRSS2, and thus can evade the intrabody SARS-CoV-2infection. This may represent an additional benefit for the application of MSC therapy in critically ill COVID-19 patients, reversing in this way the manifestation of the current disease.

MSCs may also be utilized efficiently in the recovery phase of COVID-19 patients. COVID-19 patients are suffering from extensive lung fibrosis and multiorgan damage of variable severity. Importantly, MSCs after their IV infusion: (1) Are initially distributed widespread in the body through the systemic circulation; (2) accumulate early in the lungs and then in the spleen and liver; (3) migrate to the injury or inflamed sites; and (4) finally persist to the migrated tissue for a short time before their clearance[32]. In such a way, and due to accumulation in the lung capillary network, MSCs can give rise to differentiated cells such as endothelial and epithelial cells, which can replace the damaged tissue[32]. The latter may be translated to less required recovery time for COVID-19 patients.

Considering the results of this study, MSCs may represent an important therapeutic tool for clinicians, as they can exert drastic key immunoregulatory and tissue regenerative properties. Alongside the modern therapeutic strategies, MSCs can be considered as an advanced cellular therapy, which can be applied, besides COVID-19, to other immune-related disorders such as autoimmune diseases.

ARTICLE HIGHLIGHTS

Research background

Severe acute respiratory syndrome coronavirus 2 (SARS-CoV-2) is responsible for the coronavirus disease 2019 (COVID-19) pandemic, which was initiated in December 2019. COVID-19 is characterized by a low mortality rate (< 6%); however, this percentage is higher in elderly people and patients with underlying disorders. COVID-19 is characterized by mild to severe outcomes. Currently, several therapeutic strategies have been evaluated, such as the use of anti-viral drugs, prophylactic treatment, monoclonal antibodies, and vaccination. Advanced cellular therapies are also investigated, thus representing an additional therapeutic tool for clinicians. Mesenchymal stromal cells (MSCs), which are known for their immunoregulatory properties, may halt the induced cytokine release syndrome mediated by SARS-CoV-2, and can be considered as a potential stem cell therapy.

Research motivation

Currently, a great number of clinical trials, which include the intravenous infusion of MSCs in COVID-19 patients, are performed worldwide. Preliminary data of those studies are providing encouraging results regarding the application of MSCs for better management of COVID-19. However, the exact mechanisms by which MSCs exert their beneficial properties is not fully understand. Moreover, the majority of the currently performed studies are focusing primarily to the final outcome. In this study, an initial evaluation of the immunoregulatory properties of MSCs stimulated by COVID-19 patient serum was performed. The results of this study will provide significant insights into the role of MSCs as novel immunoregulatory players.

Research objectives

The main objective of this study was to evaluate the immunoregulatory properties of WJ and BM-MSCs, which may be used as a potential advanced cellular therapy against COVID-19. The secondary objectives were to determine any discrepancies between WJ- and BM-MSCs regarding the secretion of the immunoregulatory agents (such as cytokines and growth factors) and their ability to perform M2 phenotype switch of macrophages derived from COVID-19 patients.

Research methods

Initially, WJ and BM-MSCs were isolated, expanded, and characterized according to the criteria provided by the ISCT. Then, stimulation of MSCs with a culture medium containing COVID-19 patient serum was performed. After 48 h, the COVID-19 culture medium was removed, and extensive washes of MSCs cultures were performed. Finally, new culture medium (without FBS) was added for another 48 h. Cytokine levels (IL-1Ra, IL-6, IL-10, and IL-13), growth factor levels (TGF-β1, FGF, VEGF, and PDGF), and the immunoregulatory molecule (IDO) were measured in the conditioned medium of stimulated MSCs. Also, using molecular and protein assays, the HLA-G isoforms (HLA-G1, G5, and G7) were determined. Finally, the ability of stimulated WJ and BM-MSCs to modulate the M2 macrophage phenotype was also investigated.

Research results

WJ and BM-MSCs were successfully expanded and characterized, before the performance of the stimulation experiments. MSCs from both sources exhibited a spindle-shaped morphology and successfully expressed CD73, CD90, CD105, CD29, and CD340, but did not express CD34 or CD45.

Furthermore, MSCS were successfully differentiated to "osteocytes", "chondrocytes", and "adipocytes", and therefore fulfilled the minimum criteria as defined by the ISCT. Then, the well-defined MSCs were stimulated with culture medium containing COVID-19 patient serum. Stimulated WJ and B-MSCs expressed increased levels of IL-1Ra, IL-6, IL-10, and IL-13 ($P < 0.05$) compared to unstimulated MSCs. Also, increased levels of TGF-β1, FGF, VEGF, and PDGF were observed in stimulated MSCs (from both sources) in comparison to the control group ($P < 0.05$). Co-culturing experiments of stimulated MSCs with macrophages obtained from COVID-19 patients showed the successful switch towards the M2 phenotype. Interestingly, M2 macrophages were characterized by high levels of CD206 and CD29 and low level of CD80, while CD11b was stable expressed.

Research conclusions

MSCs were successfully activated by COVID-19 patient serum and secreted anti-inflammatory cytokines and growth factors, in response towards to the initial stimuli. It has been shown that this specific set of anti-inflammatory cytokines and growth factors can efficiently modulate the overactivated immune responses in a paracrine manner. In this way, the "cytokine storm" may be halted in critically ill COVID-19 patients. Besides that, MSCs can exert key regenerative properties and thus can reverse the lung alveolar damage. This study provided evidence regarding the beneficial application of MSCs in immune-related disorders such as COVID-19.

Research perspectives

The next step of this study will be focused on performing more experiments under both *in vitro* and *in vivo* conditions. Specifically, the RNA-seq and proteomic analysis in unstimulated and stimulated WJ and BM-MSCs will provide further evidence regarding the differentially expressed proteins. Furthermore, the infusion of stimulated MSCs in animal models exhibiting acute respiratory distress syndrome will provide significant data for their immunoregulatory properties. To this direction, well-defined MSCs may represent an additional therapeutic tool for critically ill COVID-19 patients.

FOOTNOTES

Author contributions: Mallis P designed the study, performed the experimental procedures and statistical analysis, and prepared the whole manuscript; Sarri EF, Dimou Z, and Georgiou E contributed to performing the experimental procedures; Salagianni M and Triantafyllia V contributed to performing the experimental procedures and data analysis; Michalopoulos E, Chatzistamatiou T, and Andreakos E made critical revisions related to the content of the manuscript; Stavropoulos-Giokas C and Michalopoulos E performed the final approval of the manuscript.

Institutional review board statement: The overall study has received approval from the Institution's ethical board (Reference No. 1754, January 21, 2021).

Informed consent statement: The patient's legal guardian provided informed written consent prior to study enrollment.

Conflict-of-interest statement: All authors declare no conflict of interest for the current study.

Data sharing statement: No additional data are available.

Country/Territory of origin: Greece

ORCID number: Panagiotis Mallis 0000-0001-9429-190X; Theofanis Chatzistamatiou 0000-0003-4895-0155; Zetta Dimou 0000-0003-2721-0780; Eirini-Faidra Sarri 0000-0002-5185-0879; Eleni Georgiou 0000-0001-6446-2069; Maria Salagianni 0000-0001-9821-1559; Vasiliki Triantafyllia 0000-0001-5832-4014; Evangelos Andreakos 0000-0001-5536-1661; Catherine Stavropoulos-Giokas 0000-0003-0698-6061; Efstathios Michalopoulos 0000-0002-1901-6294.

Corresponding Author's Membership in Professional Societies: European Federation of Immunogenetics, No. 2527; EFIS Young Immunologist Task Force (yEFIS); Hellenic Society of Immunology; Hellenic Society of Biochemistry and Molecular Biology.

S-Editor: Xing YX
L-Editor: Wang TQ
P-Editor: Xing YX

REFERENCES

1 **Lu H**, Stratton CW, Tang YW. Outbreak of pneumonia of unknown etiology in Wuhan, China: The mystery and the miracle. *J Med Virol* 2020; **92**: 401-402 [PMID: 31950516 DOI: 10.1002/jmv.25678]

2 **Coronaviridae Study Group of the International Committee on Taxonomy of Viruses**. The species Severe acute respiratory syndrome-related coronavirus: classifying 2019-nCoV and naming it SARS-CoV-2. *Nat Microbiol* 2020; **5**: 536-544 [PMID: 32123347 DOI: 10.1038/s41564-020-0695-z]

3 **Lai CC**, Shih TP, Ko WC, Tang HJ, Hsueh PR. Severe acute respiratory syndrome coronavirus 2 (SARS-CoV-2) and coronavirus disease-2019 (COVID-19): The epidemic and the challenges. *Int J Antimicrob Agents* 2020; **55**: 105924 [PMID: 32081636 DOI: 10.1016/j.ijantimicag.2020.105924]

4 **Nature**. Why did the world's pandemic warning system fail when COVID hit? [cited 19 October 2021]. Available from: https://www.nature.com/articles/d41586-021-00162-4

5 **Jee Y**. WHO International Health Regulations Emergency Committee for the COVID-19 outbreak. *Epidemiol Health* 2020; **42**: e2020013 [PMID: 32192278 DOI: 10.4178/epih.e2020013]

6 **Johns Hopkins University of Medicine**. COVID-19 Map. 2020 [cited 7 May 2020]. Available from: https://coronavirus.jhu.edu/map.html

7 **Gebru AA**, Birhanu T, Wendimu E, Ayalew AF, Mulat S, Abasimel HZ, Kazemi A, Tadesse BA, Gebru BA, Deriba BS, Zeleke NS, Girma AG, Munkhbat B, Yusuf QK, Luke AO, Hailu D. Global burden of COVID-19: Situational analyis and review. *Hum Antibodies* 2021; **29**: 139-148 [PMID: 32804122 DOI: 10.3233/HAB-200420]

8 **Naqvi AAT**, Fatima K, Mohammad T, Fatima U, Singh IK, Singh A, Atif SM, Hariprasad G, Hasan GM, Hassan MI. Insights into SARS-CoV-2 genome, structure, evolution, pathogenesis and therapies: Structural genomics approach. *Biochim Biophys Acta Mol Basis Dis* 2020; **1866**: 165878 [PMID: 32544429 DOI: 10.1016/j.bbadis.2020.165878]

9 **Lotfi M**, Rezaei N. SARS-CoV-2: A comprehensive review from pathogenicity of the virus to clinical consequences. *J Med Virol* 2020; **92**: 1864-1874 [PMID: 32492197 DOI: 10.1002/jmv.26123]

10 **Parasher A**. COVID-19: Current understanding of its Pathophysiology, Clinical presentation and Treatment. *Postgrad Med J* 2021; **97**: 312-320 [PMID: 32978337 DOI: 10.1136/postgradmedj-2020-138577]

11 **Lotfi M**, Hamblin MR, Rezaei N. COVID-19: Transmission, prevention, and potential therapeutic opportunities. *Clin Chim Acta* 2020; **508**: 254-266 [PMID: 32474009 DOI: 10.1016/j.cca.2020.05.044]

12 **Yesudhas D**, Srivastava A, Gromiha MM. COVID-19 outbreak: history, mechanism, transmission, structural studies and therapeutics. *Infection* 2021; **49**: 199-213 [PMID: 32886331 DOI: 10.1007/s15010-020-01516-2]

13 **Paces J**, Strizova Z, Smrz D, Cerny J. COVID-19 and the immune system. *Physiol Res* 2020; **69**: 379-388 [PMID: 32469225 DOI: 10.33549/physiolres.934492]

14 **Schmitt W**, Marchiori E. Covid-19: Round and oval areas of ground-glass opacity. *Pulmonology* 2020; **26**: 246-247 [PMID: 32411942 DOI: 10.1016/j.pulmoe.2020.04.011]

15 **Hu B**, Huang S, Yin L. The cytokine storm and COVID-19. *J Med Virol* 2021; **93**: 250-256 [PMID: 32592501 DOI: 10.1002/jmv.26232]

16 **Leng Z**, Zhu R, Hou W, Feng Y, Yang Y, Han Q, Shan G, Meng F, Du D, Wang S, Fan J, Wang W, Deng L, Shi H, Li H, Hu Z, Zhang F, Gao J, Liu H, Li X, Zhao Y, Yin K, He X, Gao Z, Wang Y, Yang B, Jin R, Stambler I, Lim LW, Su H, Moskalev A, Cano A, Chakrabarti S, Min KJ, Ellison-Hughes G, Caruso C, Jin K, Zhao RC. Transplantation of ACE2^{-} Mesenchymal Stem Cells Improves the Outcome of Patients with COVID-19 Pneumonia. *Aging Dis* 2020; **11**: 216-228 [PMID: 32257537 DOI: 10.14336/AD.2020.0228]

17 **Gavriatopoulou M**, Ntanasis-Stathopoulos I, Korompoki E, Fotiou D, Migkou M, Tzanninis IG, Psaltopoulou T, Kastritis E, Terpos E, Dimopoulos MA. Emerging treatment strategies for COVID-19 infection. *Clin Exp Med* 2021; **21**: 167-179 [PMID: 33128197 DOI: 10.1007/s10238-020-00671-y]

18 **Trivedi N**, Verma A, Kumar D. Possible treatment and strategies for COVID-19: review and assessment. *Eur Rev Med Pharmacol Sci* 2020; **24**: 12593-12608 [PMID: 33336780 DOI: 10.26355/eurrev_202012_24057]

19 **Li Z**, Niu S, Guo B, Gao T, Wang L, Wang Y, Tan Y, Wu J, Hao J. Stem cell therapy for COVID-19, ARDS and pulmonary fibrosis. *Cell Prolif* 2020; **53**: e12939 [PMID: 33098357 DOI: 10.1111/cpr.12939]

20 **Shi L**, Wang L, Xu R, Zhang C, Xie Y, Liu K, Li T, Hu W, Zhen C, Wang FS. Mesenchymal stem cell therapy for severe COVID-19. *Signal Transduct Target Ther* 2021; **6**: 339 [PMID: 34497264 DOI: 10.1038/s41392-021-00754-6]

21 **Bianco P**, Robey PG, Simmons PJ. Mesenchymal stem cells: revisiting history, concepts, and assays. *Cell Stem Cell* 2008; **2**: 313-319 [PMID: 18397751 DOI: 10.1016/j.stem.2008.03.002]

22 **Mallis P**, Michalopoulos E, Chatzistamatiou T, Giokas CS. Interplay between mesenchymal stromal cells and immune system: clinical applications in immune-related diseases. *Explor Immunol* 2021; **1**: 112-139 [DOI: 10.37349/ei.2021.00010]

23 **Dominici M**, Le Blanc K, Mueller I, Slaper-Cortenbach I, Marini F, Krause D, Deans R, Keating A, Prockop Dj, Horwitz E. Minimal criteria for defining multipotent mesenchymal stromal cells. The International Society for Cellular Therapy position statement. *Cytotherapy* 2006; **8**: 315-317 [PMID: 16923606 DOI: 10.1080/14653240600855905]

24 **Viswanathan S**, Shi Y, Galipeau J, Krampera M, Leblanc K, Martin I, Nolta J, Phinney DG, Sensebe L. Mesenchymal stem *vs* stromal cells: International Society for Cell & Gene Therapy (ISCT®) Mesenchymal Stromal Cell committee position statement on nomenclature. *Cytotherapy* 2019; **21**: 1019-1024 [PMID: 31526643 DOI: 10.1016/j.jcyt.2019.08.002]

25 **Griffin MD**, Ritter T, Mahon BP. Immunological aspects of allogeneic mesenchymal stem cell therapies. *Hum Gene Ther* 2010; **21**: 1641-1655 [PMID: 20718666 DOI: 10.1089/hum.2010.156]

26 **Machado Cde V**, Telles PD, Nascimento IL. Immunological characteristics of mesenchymal stem cells. *Rev Bras Hematol Hemoter* 2013; **35**: 62-67 [PMID: 23580887 DOI: 10.5581/1516-8484.20130017]

27 **Via AG**, Frizziero A, Oliva F. Biological properties of mesenchymal Stem Cells from different sources. *Muscles Ligaments Tendons J* 2012; **2**: 154-162 [PMID: 23738292]

28 **Chen JY**, Mou XZ, Du XC, Xiang C. Comparative analysis of biological characteristics of adult mesenchymal stem cells with different tissue origins. *Asian Pac J Trop Med* 2015; **8**: 739-746 [PMID: 26433660 DOI: 10.1016/j.apjtm.2015.07.022]

29 **Stewart MC**, Stewart AA. Mesenchymal stem cells: characteristics, sources, and mechanisms of action. *Vet Clin North Am Equine Pract* 2011; **27**: 243-261 [PMID: 21872757 DOI: 10.1016/j.cveq.2011.06.004]

30 **Yi T**, Song SU. Immunomodulatory properties of mesenchymal stem cells and their therapeutic applications. *Arch Pharm Res* 2012; **35**: 213-221 [PMID: 22370776 DOI: 10.1007/s12272-012-0202-z]

31 **Mallis P**, Michalopoulos E, Chatzistamatiou T, Stavropoulos-Giokas C. Mesenchymal stromal cells as potential immunomodulatory players in severe acute respiratory distress syndrome induced by SARS-CoV-2 infection. *World J Stem Cells* 2020; **12**: 731-751 [PMID: 32952855 DOI: 10.4252/wjsc.v12.i8.731]

32 **da Silva KN**, Gobatto ALN, Costa-Ferro ZSM, Cavalcante BRR, Caria ACI, de Aragão França LS, Nonaka CKV, de Macêdo Lima F, Lopes-Pacheco M, Rocco PRM, de Freitas Souza BS. Is there a place for mesenchymal stromal cell-based therapies in the therapeutic armamentarium against COVID-19? *Stem Cell Res Ther* 2021; **12**: 425 [PMID: 34315546 DOI: 10.1186/s13287-021-02502-7]

33 **Meng F**, Xu R, Wang S, Xu Z, Zhang C, Li Y, Yang T, Shi L, Fu J, Jiang T, Huang L, Zhao P, Yuan X, Fan X, Zhang JY, Song J, Zhang D, Jiao Y, Liu L, Zhou C, Maeurer M, Zumla A, Shi M, Wang FS. Human umbilical cord-derived mesenchymal stem cell therapy in patients with COVID-19: a phase 1 clinical trial. *Signal Transduct Target Ther*. 2020; **5**: 172 [PMID: 32855385 DOI: 10.1038/s41392-020-00286-5]

34 **Saleh M**, Vaezi AA, Aliannejad R, Sohrabpour AA, Kiaei SZF, Shadnoush M, Siavashi V, Aghaghazvini L, Khoundabi B, Abdoli S, Chahardouli B, Seyhoun I, Alijani N, Verdi J. Cell therapy in patients with COVID-19 using Wharton's jelly mesenchymal stem cells: a phase 1 clinical trial. *Stem Cell Res Ther* 2021; **12**: 410 [PMID: 34271988 DOI: 10.1186/s13287-021-02483-7]

35 **Sharma D**, Zhao F. Updates on clinical trials evaluating the regenerative potential of allogenic mesenchymal stem cells in COVID-19. *NPJ Regen Med* 2021; **6**: 37 [PMID: 34193864 DOI: 10.1038/s41536-021-00147-x]

36 **Payares-Herrera C**, Martínez-Muñoz ME, Vallhonrat IL, de Molina RM, Torres MP, Trisan A, de Diego IS, Alonso R, Zafra R, Donaire T, Sánchez R, Rubio JJ, Duarte Palomino RF, Solá CA. Double-blind, randomized, controlled, trial to assess the efficacy of allogenic mesenchymal stromal cells in patients with acute respiratory distress syndrome due to COVID-19 (COVID-AT): A structured summary of a study protocol for a randomised controlled trial. *Trials* 2021; **22**: 9 [PMID: 33407777 DOI: 10.1186/s13063-020-04964-1]

37 **Shetty AK**, Shetty PA, Zanirati G, Jin K. Further validation of the efficacy of mesenchymal stem cell infusions for reducing mortality in COVID-19 patients with ARDS. *NPJ Regen Med* 2021; **6**: 53 [PMID: 34504110 DOI: 10.1038/s41536-021-00161-z]

38 **Bühring HJ**, Battula VL, Treml S, Schewe B, Kanz L, Vogel W. Novel markers for the prospective isolation of human MSC. *Ann N Y Acad Sci* 2007; **1106**: 262-271 [PMID: 17395729 DOI: 10.1196/annals.1392.000]

39 **Kim M**, Bae YK, Um S, Kwon JH, Kim GH, Choi SJ, Oh W, Jin HJ. A Small-Sized Population of Human Umbilical Cord Blood-Derived Mesenchymal Stem Cells Shows High Stemness Properties and Therapeutic Benefit. *Stem Cells Int* 2020; **2020**: 5924983 [PMID: 32399043 DOI: 10.1155/2020/5924983]

40 **Hunt JS**, Petroff MG, McIntire RH, Ober C. HLA-G and immune tolerance in pregnancy. *FASEB J* 2005; **19**: 681-693 [PMID: 15857883 DOI: 10.1096/fj.04-2078rev]

41 **Yen BL**, Hwa HL, Hsu PJ, Chen PM, Wang LT, Jiang SS, Liu KJ, Sytwu HK, Yen ML. HLA-G Expression in Human Mesenchymal Stem Cells (MSCs) Is Related to Unique Methylation Pattern in the Proximal Promoter as well as Gene Body DNA. *Int J Mol Sci* 2020; **21** [PMID: 32708387 DOI: 10.3390/ijms21145075]

42 **Rizzo R**, Lanzoni G, Stignani M, Campioni D, Alviano F, Ricci F, Tazzari PL, Melchiorri L, Scalinci SZ, Cuneo A, Bonsi L, Lanza F, Bagnara GP, Baricordi OR. A simple method for identifying bone marrow mesenchymal stromal cells with a high immunosuppressive potential. *Cytotherapy* 2011; **13**: 523-527 [PMID: 21171826 DOI: 10.3109/14653249.2010.542460]

43 **Rizzo R**, Campioni D, Stignani M, Melchiorri L, Bagnara GP, Bonsi L, Alviano F, Lanzoni G, Moretti S, Cuneo A, Lanza F, Baricordi OR. A functional role for soluble HLA-G antigens in immune modulation mediated by mesenchymal stromal cells. Cytotherapy. 2008;10 :364-75. [PMID: 18574769 DOI: 10.1080/14653240802105299]

44 **Montespan F**, Deschaseaux F, Sensébé L, Carosella ED, Rouas-Freiss N. Osteodifferentiated mesenchymal stem cells from bone marrow and adipose tissue express HLA-G and display immunomodulatory properties in HLA-mismatched settings: implications in bone repair therapy. *J Immunol Res* 2014; **2014**: 230346 [PMID: 24877156 DOI: 10.1155/2014/230346]

45 **Mallis P**, Boulari D, Michalopoulos E, Dinou A, Spyropoulou-Vlachou M, Stavropoulos-Giokas C. Evaluation of HLA-G Expression in Multipotent Mesenchymal Stromal Cells Derived from Vitrified Wharton's Jelly Tissue. *Bioengineering (Basel)* 2018; **5** [PMID: 30388848 DOI: 10.3390/bioengineering5040095]

46 **Ding DC**, Chou HL, Chang YH, Hung WT, Liu HW, Chu TY. Characterization of HLA-G and Related Immunosuppressive Effects in Human Umbilical Cord Stroma-Derived Stem Cells. *Cell Transplant* 2016; **25**: 217-228 [PMID: 26044082 DOI: 10.3727/096368915X688182]

47 **Venkatesha SH**, Dudics S, Acharya B, Moudgil KD. Cytokine-modulating strategies and newer cytokine targets for arthritis therapy. *Int J Mol Sci* 2014; **16**: 887-906 [PMID: 25561237 DOI: 10.3390/ijms16010887]

48 **Koorts AM**, Levay PF, Becker PJ, Viljoen M. Pro- and anti-inflammatory cytokines during immune stimulation: modulation of iron status and red blood cell profile. *Mediators Inflamm* 2011; **2011**: 716301 [PMID: 21547258 DOI: 10.1155/2011/716301]

49 **Sanjabi S**, Zenewicz LA, Kamanaka M, Flavell RA. Anti-inflammatory and pro-inflammatory roles of TGF-beta, IL-10, and IL-22 in immunity and autoimmunity. *Curr Opin Pharmacol* 2009; **9**: 447-453 [PMID: 19481975 DOI: 10.1016/j.coph.2009.04.008]

50 **Arend WP**, Malyak M, Guthridge CJ, Gabay C. Interleukin-1 receptor antagonist: role in biology. *Annu Rev Immunol* 1998; **16**: 27-55 [PMID: 9597123 DOI: 10.1146/annurev.immunol.16.1.27]

51 **Dayer JM**. [Biological modulation of IL-1 activity: role and development of its natural inhibitor IL-1Ra]. *Reumatismo* 2004; **56**: 3-8 [PMID: 15201935]

52 **Bustos ML**, Huleihel L, Meyer EM, Donnenberg AD, Donnenberg VS, Sciurba JD, Mroz L, McVerry BJ, Ellis BM, Kaminski N, Rojas M. Activation of human mesenchymal stem cells impacts their therapeutic abilities in lung injury by increasing interleukin (IL)-10 and IL-1RN levels. *Stem Cells Transl Med* 2013; **2**: 884-895 [PMID: 24089414 DOI: 10.5966/sctm.2013-0033]

53 **Couper KN**, Blount DG, Riley EM. IL-10: the master regulator of immunity to infection. *J Immunol* 2008; **180**: 5771-5777 [PMID: 18424693 DOI: 10.4049/jimmunol.180.9.5771]

54 **Hershey GK**. IL-13 receptors and signaling pathways: an evolving web. *J Allergy Clin Immunol* 2003; **111**: 677-90; quiz 691 [PMID: 12704343 DOI: 10.1067/mai.2003.1333]

55 **Bhattacharjee A**, Shukla M, Yakubenko VP, Mulya A, Kundu S, Cathcart MK. IL-4 and IL-13 employ discrete signaling pathways for target gene expression in alternatively activated monocytes/macrophages. *Free Radic Biol Med* 2013; **54**: 1-16 [PMID: 23124025 DOI: 10.1016/j.freeradbiomed.2012.10.553]

56 **Martinez-Nunez RT**, Louafi F, Sanchez-Elsner T. The interleukin 13 (IL-13) pathway in human macrophages is modulated by microRNA-155 *via* direct targeting of interleukin 13 receptor alpha1 (IL13Ralpha1). *J Biol Chem* 2011; **286**: 1786-1794 [PMID: 21097505 DOI: 10.1074/jbc.M110.169367]

57 **Huang XL**, Wang YJ, Yan JW, Wan YN, Chen B, Li BZ, Yang GJ, Wang J. Role of anti-inflammatory cytokines IL-4 and IL-13 in systemic sclerosis. *Inflamm Res* 2015; **64**: 151-159 [PMID: 25725697 DOI: 10.1007/s00011-015-0806-0]

58 **Tanaka T**, Narazaki M, Kishimoto T. IL-6 in inflammation, immunity, and disease. *Cold Spring Harb Perspect Biol* 2014; **6**: a016295 [PMID: 25190079 DOI: 10.1101/cshperspect.a016295]

59 **Gabay C**. Interleukin-6 and chronic inflammation. *Arthritis Res Ther* 2006; **8** Suppl 2: S3 [PMID: 16899107 DOI: 10.1186/ar1917]

60 **Galani IE**, Rovina N, Lampropoulou V, Triantafyllia V, Manioudaki M, Pavlos E, Koukaki E, Fragkou PC, Panou V, Rapti V, Koltsida O, Mentis A, Koulouris N, Tsiodras S, Koutsoukou A, Andreakos E. Untuned antiviral immunity in COVID-19 revealed by temporal type I/III interferon patterns and flu comparison. *Nat Immunol* 2021; **22**: 32-40 [PMID: 33277638 DOI: 10.1038/s41590-020-00840-x]

61 **Xing Z**, Gauldie J, Cox G, Baumann H, Jordana M, Lei XF, Achong MK. IL-6 is an antiinflammatory cytokine required for controlling local or systemic acute inflammatory responses. *J Clin Invest* 1998; **101**: 311-320 [PMID: 9435302 DOI: 10.1172/JCI1368]

62 **Jones SA**. Directing transition from innate to acquired immunity: defining a role for IL-6. *J Immunol* 2005; **175**: 3463-3468 [PMID: 16148087 DOI: 10.4049/jimmunol.175.6.3463]

63 **Steensberg A**, Fischer CP, Keller C, Møller K, Pedersen BK. IL-6 enhances plasma IL-1ra, IL-10, and cortisol in humans. *Am J Physiol Endocrinol Metab* 2003; **285**: E433-E437 [PMID: 12857678 DOI: 10.1152/ajpendo.00074.2003]

64 **Dorronsoro A**, Lang V, Ferrin I, Fernández-Rueda J, Zabaleta L, Pérez-Ruiz E, Sepúlveda P, Trigueros C. Intracellular role of IL-6 in mesenchymal stromal cell immunosuppression and proliferation. *Sci Rep* 2020; **10**: 21853 [PMID: 33318571 DOI: 10.1038/s41598-020-78864-4]

65 **Wang G**, Cao K, Liu K, Xue Y, Roberts AI, Li F, Han Y, Rabson AB, Wang Y, Shi Y. Kynurenic acid, an IDO metabolite, controls TSG-6-mediated immunosuppression of human mesenchymal stem cells. *Cell Death Differ* 2018; **25**: 1209-1223 [PMID: 29238069 DOI: 10.1038/s41418-017-0006-2]

66 **Mellor AL**, Keskin DB, Johnson T, Chandler P, Munn DH. Cells expressing indoleamine 2,3-dioxygenase inhibit T cell responses. *J Immunol* 2002; **168**: 3771-3776 [PMID: 11937528 DOI: 10.4049/jimmunol.168.8.3771]

67 **Munn DH**, Shafizadeh E, Attwood JT, Bondarev I, Pashine A, Mellor AL. Inhibition of T cell proliferation by macrophage tryptophan catabolism. *J Exp Med* 1999; **189**: 1363-1372 [PMID: 10224276 DOI: 10.1084/jem.189.9.1363]

68 **Black AR**, Black JD. Protein kinase C signaling and cell cycle regulation. *Front Immunol* 2012; **3**: 423 [PMID: 23335926 DOI: 10.3389/fimmu.2012.00423]

69 **Jones SM**, Kazlauskas A. Connecting signaling and cell cycle progression in growth factor-stimulated cells. *Oncogene* 2000; **19**: 5558-5567 [PMID: 11114735 DOI: 10.1038/sj.onc.1203858]

70 **Jones SM**, Kazlauskas A. Growth factor-dependent signaling and cell cycle progression. *FEBS Lett* 2001; **490**: 110-116 [PMID: 11223025 DOI: 10.1016/s0014-5793(01)02113-5]

71 **Tabata Y**. Tissue regeneration based on growth factor release. *Tissue Eng* 2003; **9** Suppl 1: S5-15 [PMID: 14511467 DOI: 10.1089/10763270360696941]

72 **Kulebyakin KY**, Nimiritsky PP, Makarevich PI. Growth Factors in Regeneration and Regenerative Medicine: "the Cure and the Cause". *Front Endocrinol (Lausanne)* 2020; **11**: 384 [PMID: 32733378 DOI: 10.3389/fendo.2020.00384]

73 **Vasandan AB**, Jahnavi S, Shashank C, Prasad P, Kumar A, Prasanna SJ. Human Mesenchymal stem cells program macrophage plasticity by altering their metabolic status *via* a PGE_2-dependent mechanism. *Sci Rep* 2016; **6**: 38308 [PMID: 27910911 DOI: 10.1038/srep38308]

74 **Jin L**, Deng Z, Zhang J, Yang C, Liu J, Han W, Ye P, Si Y, Chen G. Mesenchymal stem cells promote type 2 macrophage polarization to ameliorate the myocardial injury caused by diabetic cardiomyopathy. *J Transl Med* 2019; **17**: 251 [PMID: 31382970 DOI: 10.1186/s12967-019-1999-8]

75 **Barros MH**, Hauck F, Dreyer JH, Kempkes B, Niedobitek G. Macrophage polarisation: an immunohistochemical approach for identifying M1 and M2 macrophages. *PLoS One* 2013; **8**: e80908 [PMID: 24260507 DOI: 10.1371/journal.pone.0080908]

76 **Hu JM**, Liu K, Liu JH, Jiang XL, Wang XL, Chen YZ, Li SG, Zou H, Pang LJ, Liu CX, Cui XB, Yang L, Zhao J, Shen XH, Jiang JF, Liang WH, Yuan XL, Li F. CD163 as a marker of M2 macrophage, contribute to predicte aggressiveness and prognosis of Kazakh esophageal squamous cell carcinoma. *Oncotarget* 2017; **8**: 21526-21538 [PMID: 28423526 DOI: 10.18632/oncotarget.15630]

77 **Cao X**, Yakala GK, van den Hil FE, Cochrane A, Mummery CL, Orlova VV. Differentiation and Functional Comparison of Monocytes and Macrophages from hiPSCs with Peripheral Blood Derivatives. *Stem Cell Reports* 2019; **12**: 1282-1297 [PMID: 31189095 DOI: 10.1016/j.stemcr.2019.05.003]

78 **Ammon C**, Meyer SP, Schwarzfischer L, Krause SW, Andreesen R, Kreutz M. Comparative analysis of integrin expression on monocyte-derived macrophages and monocyte-derived dendritic cells. *Immunology* 2000; **100**: 364-369 [PMID: 10929059 DOI: 10.1046/j.1365-2567.2000.00056.x]

79 **Domenis R**, Cifù A, Quaglia S, Pistis C, Moretti M, Vicario A, Parodi PC, Fabris M, Niazi KR, Soon-Shiong P, Curcio F. Pro inflammatory stimuli enhance the immunosuppressive functions of adipose mesenchymal stem cells-derived exosomes. *Sci Rep* 2018; **8**: 13325 [PMID: 30190615 DOI: 10.1038/s41598-018-31707-9]

80 **de Witte SFH**, Luk F, Sierra Parraga JM, Gargesha M, Merino A, Korevaar SS, Shankar AS, O'Flynn L, Elliman SJ, Roy D, Betjes MGH, Newsome PN, Baan CC, Hoogduijn MJ. Immunomodulation By Therapeutic Mesenchymal Stromal Cells (MSC) Is Triggered Through Phagocytosis of MSC By Monocytic Cells. *Stem Cells* 2018; **36**: 602-615 [PMID: 29341339 DOI: 10.1002/stem.2779]

81 **Weiss ARR**, Dahlke MH. Immunomodulation by Mesenchymal Stem Cells (MSCs): Mechanisms of Action of Living, Apoptotic, and Dead MSCs. *Front Immunol* 2019; **10**: 1191 [PMID: 31214172 DOI: 10.3389/fimmu.2019.01191]

82 **Shi L**, Yuan W, Wang S, Zhang C, Zhang B, Song J, Huang L, Xu Z, Fu JL, Li Y, Xu R, Li TT, Dong J, Cai J, Li G, Xie Y, Shi M, Zhang Y, Xie WF, Wang FS. Human Mesenchymal Stem Cells Treatment for severe COVID-19: 1-year follow-up results of a randomized, double blind, placebo control trial. EBioMedicine 2022; 75: 103789 [PMID: 34963099 DOI: 10.1016/j.ebiom.2021.103789]

83 **Gallelli L**, Zhang L, Wang T, Fu F. Severe Acute Lung Injury Related to COVID-19 Infection: A Review and the Possible Role for Escin. *J Clin Pharmacol* 2020; **60**: 815-825 [PMID: 32441805 DOI: 10.1002/jcph.1644]

84 **Avanzini MA**, Mura M, Percivalle E, Bastaroli F, Croce S, Valsecchi C, Lenta E, Nykjaer G, Cassaniti I, Bagnarino J, Baldanti F, Zecca M, Comoli P, Gnecchi M. Human mesenchymal stromal cells do not express ACE2 and TMPRSS2 and are not permissive to SARS-CoV-2 infection. *Stem Cells Transl Med* 2021; **10**: 636-642 [PMID: 33188579 DOI: 10.1002/sctm.20-0385]

Published by **Baishideng Publishing Group Inc**
7041 Koll Center Parkway, Suite 160, Pleasanton, CA 94566, USA
Telephone: +1-925-3991568
E-mail: bpgoffice@wjgnet.com
Help Desk: https://www.f6publishing.com/helpdesk
https://www.wjgnet.com